AD-A147 425 FRAZIL ICE FORMATION(U) IOWA INST OF HYDRAULIC RESEARCH 1/1
IOWA CITY R ETTEMA ET AL. JUL 84 CRREL-84-18
DACA89-79-C-0010

UNCLASSIFIED F/G 8/12 NL

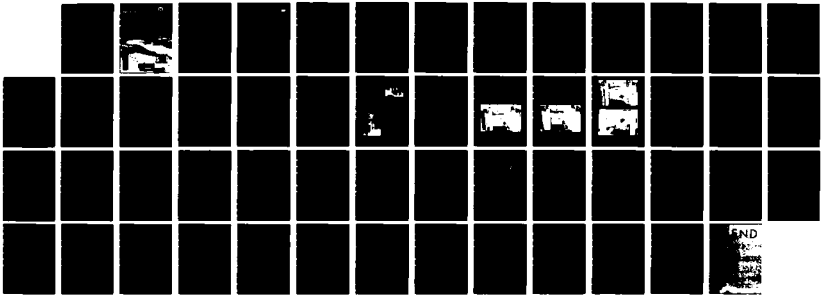

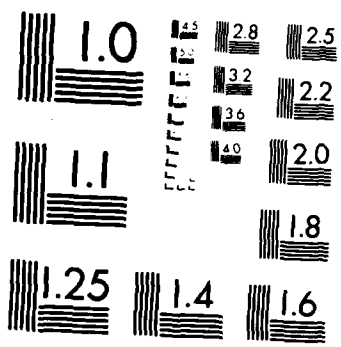

CRREL
REPORT 84-18

(12)

US Army Corps of Engineers
Cold Regions Research & Engineering Laboratory

Frazil ice formation

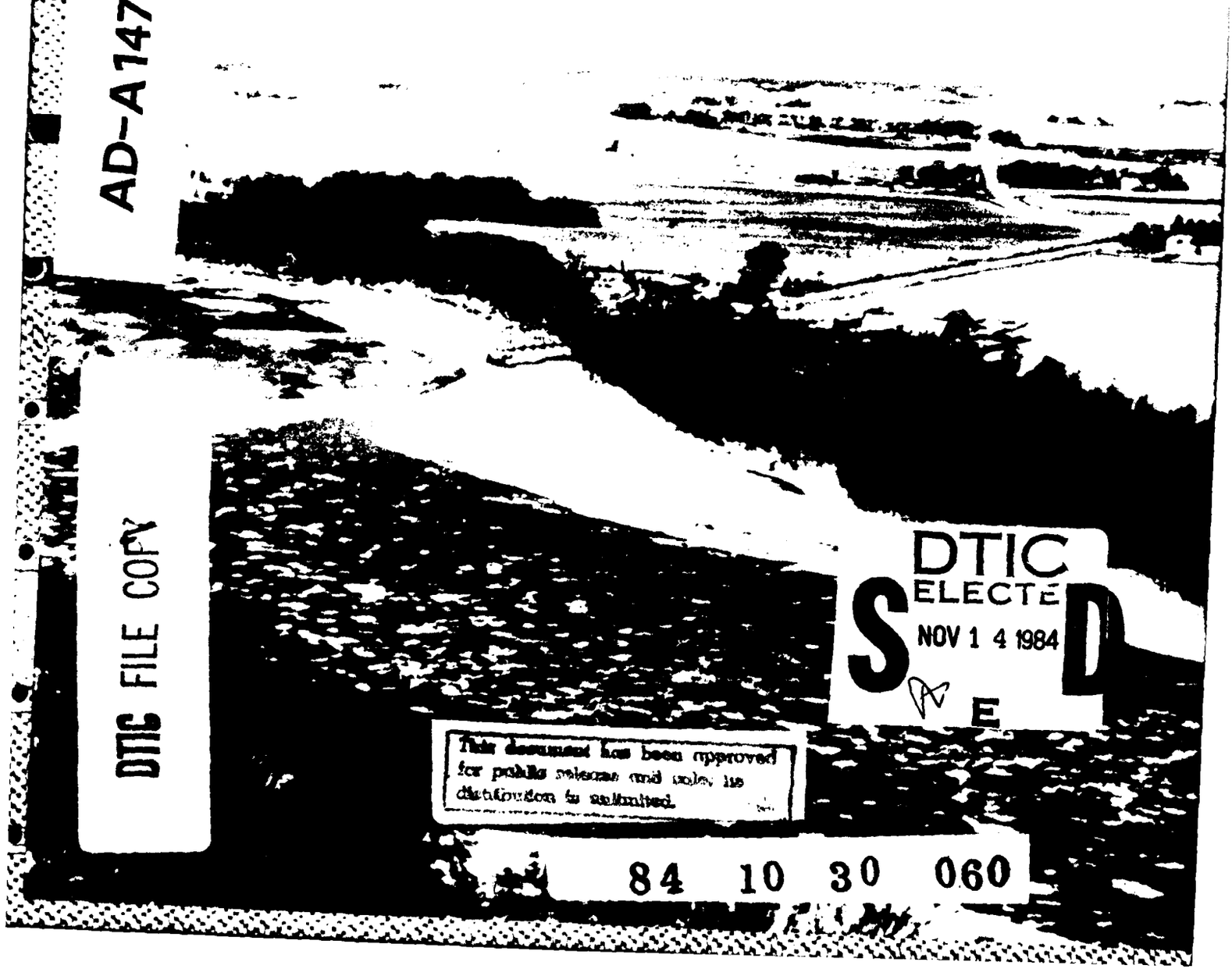

For conversion of SI metric units to U.S./British customary units of measurement consult ASTM Standard E380, Metric Practice Guide, *published by the American Society for Testing and Materials, 1916 Race St., Philadelphia, Pa. 19103.*

Cover: Frazil ice pans on the Cedar River, Iowa.

12

CRREL Report 84-18

July 1984

Frazil ice formation

R. Ettema, M.F. Karim and J.F. Kennedy

Unclassified

SECURITY CLASSIFICATION OF THIS PAGE *(When Data Entered)*

REPORT DOCUMENTATION PAGE		READ INSTRUCTIONS BEFORE COMPLETING FORM
1. REPORT NUMBER CRREL Report 84-18	2. GOVT ACCESSION NO. A147425	3. RECIPIENT'S CATALOG NUMBER
4. TITLE *(and Subtitle)* FRAZIL ICE FORMATION		5. TYPE OF REPORT & PERIOD COVERED 6. PERFORMING ORG. REPORT NUMBER
7. AUTHOR(s) R. Ettema, M.F. Karim and J.F. Kennedy		8. CONTRACT OR GRANT NUMBER(s) DACA 89-79-C-0010 and NSF Grant CEE-09252
9. PERFORMING ORGANIZATION NAME AND ADDRESS Iowa Institute of Hydraulic Research University of Iowa Iowa City, Iowa		10. PROGRAM ELEMENT, PROJECT, TASK AREA & WORK UNIT NUMBERS
11. CONTROLLING OFFICE NAME AND ADDRESS U.S. Army Cold Regions Research and Engineering Laboratory Hanover, New Hampshire 03755 and National Science Foundation, Washington, D.C.		12. REPORT DATE July 1984 13. NUMBER OF PAGES 50
14. MONITORING AGENCY NAME & ADDRESS *(if different from Controlling Office)*		15. SECURITY CLASS. *(of this report)* Unclassified 15a. DECLASSIFICATION/DOWNGRADING SCHEDULE

16. DISTRIBUTION STATEMENT *(of this Report)*

Approved for public release; distribution is unlimited.

17. DISTRIBUTION STATEMENT *(of the abstract entered in Block 20, if different from Report)*

18. SUPPLEMENTARY NOTES

19. KEY WORDS *(Continue on reverse side if necessary and identify by block number)*

Cold regions
Frazil ice
Ice
Ice formation
Laboratory tests
Mathematical models

20. ABSTRACT *(Continue on reverse side if necessary and identify by block number)*

This report investigates the influences of turbulence and water temperature on frazil ice formation. The rate and the quantity of frazil ice formed in a specified volume of supercooled water increase with both increasing turbulence intensity and decreasing water temperature. The influence of turbulence intensity on the rate of frazil ice formation, however, is more pronounced for larger initial supercooling. The turbulence characteristics of a flow affect the rate of frazil ice formation by governing the temperature to which the flow can be supercooled, by influencing heat transfer from the frazil ice to surrounding water, and by promoting collision nucleation, particle and floc rupture and increasing the number of nucleation sites. Larger frazil ice particles formed in water supercooled to lower temperatures. The particles usually were disks, with diameters several orders greater than their thickness. Particle size generally decreased with

DD FORM 1 JAN 73 1473 EDITION OF 1 NOV 65 IS OBSOLETE

Unclassified

SECURITY CLASSIFICATION OF THIS PAGE *(When Data Entered)*

20. Abstract (cont'd).

increasing turbulence intensity. This report develops an analytical model, in which the rate of frazil ice formation is related to temperature rise of a turbulent volume of water from the release of latent heat of fusion of liquid water to ice. Experiments conducted in a turbulence jar with a heated, vertically oscillating grid served both to guide and to calibrate the analytical model as well as to afford insights into frazil ice formation. The formation of frazil ice was studied for temperatures of supercooled water ranging from -0.9° to -0.05°C.

PREFACE

This report was prepared by Robert Ettema, Research Engineer, M. Fazle Karim, Research Engineer, and John F. Kennedy, Director, all of the Iowa Institute of Hydraulic Research, University of Iowa, Iowa City. The experimental phases of this project were funded under Grant No. DACA 89-79-C 0010 by the U.S. Army Cold Regions Research and Engineering Laboratory. Financial assistance for the analytical phases and preparation of this report was provided by National Science Foundation Grant No. CEE-09252.

This report was technically reviewed by James L. Wuebben and Steven F. Daly of CRREL.

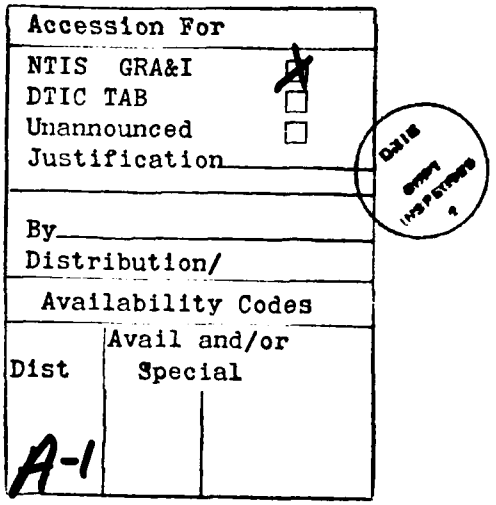

CONTENTS

ILLUSTRATIONS

TABLES

NOMENCLATURE

a	reference level
A	constant
A_o	surface area of frazil ice at time $t = 0$
A_t	surface area of frazil ice at time t
b	representative thickness of frazil ice particles
c	concentration
$\dot{c}$	temporal rate of frazil ice concentration increase
c_t	frazil ice concentration at time t
c_{max}	maximum concentration of frazil ice
c_s	sediment concentration
C_1	constant
D	flow depth
F_g	frequency of grid oscillation
k	coefficient of thermal conductivity
K	constant
L	characteristic length
L_i	latent heat of fusion
m	exponent
M_i	mass of ice
M_W	mass of water
n	exponent
n_1, n_2, n_3	constants
N	number of ice crystals
N_u	Nusselt number
N_s	rate of sediment transport
P_r	Prandtl number
Q_F	rate at which ice gives up heat of fusion
Q_h	rate of heat transfer to water from surroundings and grid
Q_i	heat flux from channel bed to water
Q_s	rate of heat loss from water surface
Q_w	rate of heat uptake by water
R_e	Reynolds number
S	concentration versus depth curve slope
S_H	specific heat of water
t	time
t_n	time of first nucleation
T	water temperature
T_m	equilibrium temperature of liquid water and ice
T_o	temperature of supercooling at time $t = 0$
$\dot{T}$	rate of temperature rise because of heated grid and surroundings of the jar
$\dot{T}_{frazil}$	average temporal rate of temperature rise because of frazil ice formation
v	characteristic velocity of flow
V	volume of water in the jar
w	fall velocity
x	$T-T_m$
y	elevation in fluid
α	heat transfer coefficient
α_o	α at time $t = 0$
β	constant
ϵ	turbulence exchange coefficient
ℓ	characteristic width scale
ℓ_p	Prandtl mixing length
ρ	density of water
ρ_i	density of ice
υ	kinematic viscosity

FRAZIL ICE FORMATION

R. Ettema, M.F. Karim and J.F. Kennedy

INTRODUCTION

Background

Frazil ice forms in flowing or turbulent water that has become supercooled by heat transfer to overlying air. Turbulence, by agitating the water surface or the water-air interface, inhibits the growth of a monolithic ice sheet. The principal phases of frazil ice growth are depicted schematically in Figure 1. Ice crystals such as snow, frozen fog or ice fragments can, on entering supercooled water, initiate the formation of frazil ice. As the crystals of frazil ice form, they are entrained and transported downstream in flowing water, or are dispersed over the depth of agitated water. Once formed, small frazil ice crystals grow, agglutinate

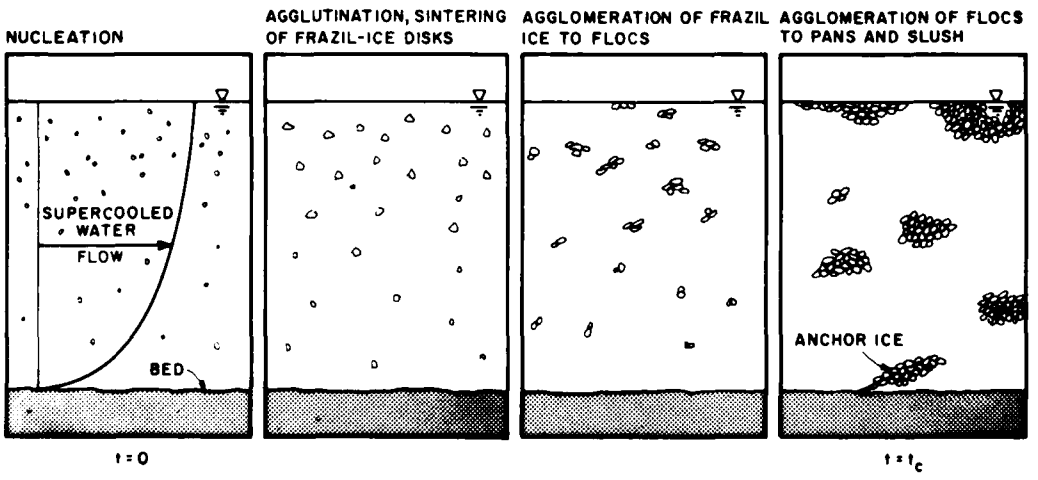

Figure 1. Phases of frazil ice formation in a stream (after Williams 1959).

to each other and may subsequently agglomerate as flocs. The buoyant flocs of frazil ice rise to the water surface where, if there is no ice cover, they accumulate to form ice pans on their exposure to the frigid air. The pans often freeze to each other and form small ice floes. The accumulation of these floes along the edge of a downstream ice cover can lead to the freeze-over of a river. When the transported flocs of frazil ice become trapped beneath an existing ice cover, slush ice may accumulate. The volume of frazil ice produced in a stream can potentially exceed the volume of surface ice produced in it.

Frazil ice is of engineering significance largely because accumulations of it can cause problems for many structures in or adjoining rivers, lakes and coastal waters in cold regions. Two prominent problems associated with frazil ice are the adherence of frazil ice to structures in water and the constriction of a stream or river flow cross section by accumulations of frazil ice beneath an ice cover. The present study directly addresses neither of these problems; instead, it deals with some of the fundamental aspects of frazil ice formation.

Scope of study

The amount of frazil ice that forms in a body of supercooled water principally depends on the degree of supercooling at the instant of seeding, nucleation dynamics and the rate of heat transfer from the water body. In nature, these factors are functions of, among other things, the turbulence characteristics of the flow. The formation of frazil ice involves processes of crystal growth, secondary nucleation or the creation of new crystals via collision breeding, and the combination of frazil ice crystals to form frazil ice particles and flocs. Three critical unresolved issues related to the formation of frazil ice are:

1. How does water temperature at seeding influence the rate of frazil ice formation?
2. How do the turbulence characteristics of a flow affect the rate of secondary nucleation and frazil ice formation?
3. How does the mean size of frazil ice particles vary with water temperature and the turbulence characteristics of the body of water?

The study reported here investigated these issues by observation of them, both experimentally in a turbulence jar and by way of an analytical model in which the rate of frazil ice formation is related to turbulence level and temperature of a body of pure water. The results from the experiments guided the formulation of the analytical model that predicts the rate of frazil ice formation for a given temperature of supercooling and turbulence exchange coefficient of a flow. River and stream waters rarely become supercooled to temperatures less than about -0.1°C. However, so that the influences of turbulence and temperature of a flow would be accentuated sufficiently to be apparent, frazil ice formation over a wider range of water temperatures, as low as -0.9°C, was studied.

The *Literature Review* section of this report briefly reviews literature pertaining to nucleation, growth and evolution of frazil ice particles in pure water. Formulation of an analytical description of frazil ice formation is outlined in the *Analytical Model* section. Experiments that are companion to the analytical model are described in the *Experimentation* section. Results from the analytical model and from experimentation are combined and discussed in the *Results* section and the principal conclusions of the study are presented in the *Conclusions* section. Appendix A is a description of frazil ice experiments that were performed in the early stage of the present investigation, but were subsequently abandoned. A computer program for solving the analytical model is listed in Appendix B and the results obtained from this analytical model are presented in Appendix C.

LITERATURE REVIEW

Introduction

The formation of frazil ice and its growth and evolution into larger ice masses in rivers, lakes, coastal waters and man-made channels pose many challenging problems for the design and operation of hydraulic structures. Understanding the mechanics of frazil ice formation has been the subject of investigation by many researchers—some of the earliest research efforts were undertaken by Barnes (1928) and Devik (1931). Altberg (1936) presented a comprehensive review of early work (1915-1935) on underwater ice formation and discussed the formation of frazil ice and anchor ice in terms of heat convection by supercooled water (anchor ice is submerged ice that is attached to the bottom of a stream or submerged objects in a stream). Tsang (1982), Martin (1981) and Osterkamp (1978a) have recently published erudite reviews of current knowledge concerning frazil ice. The present review is limited to surveying briefly the literature dealing with the salient features of frazil ice formation, namely, the influences of water temperature and turbulence on the rate of frazil ice formation and the size of frazil ice particles.

Incipient formation of frazil ice

Frazil ice forms in supercooled liquid water that is turbulent. The introduction of seed ice crystals is required to begin, by the process of secondary nucleation, the formation of frazil ice. Secondary nucleation involves the proliferation of ice crystals through the mechanism of collision and disintegration of an initial set of ice particles. Ice particles may break during collisions with each other or with other solid surfaces, or because of their impact with fluid eddies.

Depending on the rate of heat transfer to overlying air, a body of water may be further supercooled after frazil ice has begun to form, or it may begin to warm because of the release of latent heat of fusion that accompanies ice formation. In nature, the supercooling of water is usually accompanied by ice growth, either as frazil ice or an ice cover forming from the surface borders of the flow. Consequently, the supercooling of water in rivers and streams is usually limited to about 0.1°C or less below 0°C. Williams (1959), in his review of the current theories of frazil ice formation, summarized various researchers' theories of frazil ice formation. These studies dealt, to varying degrees, with the supercooling of water and the nucleation of supercooled water, and included studies concerning the factors affecting the rate of cooling in open rivers. In addition, early attempts to predict the onset and rate of frazil ice production, based on knowledge of water temperature, are outlined by Williams. The following citations paraphrase a portion of Williams' paper.

Schaefer (1950) reported that the supercooling of water in streams frequently persisted for long periods (often days) but that the water is rarely supercooled below -0.1°C. According to Dorsey (1948) the formation of frazil ice is started by ice molecules or by heterogeneous singularities—that is, foreign particles in water that serve as ice nuclei—that fall into a supercooled body of water. Kumai and Itagaki (1954) concluded from their photographic study of frazil ice formation that with a temperature of supercooling down to -0.3°C discoid and spicule frazil ice particles are produced, and from -0.6° to -0.9°C only the spicule particles are formed. Granbois (1953) reported, from his measurements in rivers, that frazil ice forms only when the rate of temperature change of the water is greater than 0.01°C/hr for temperatures of supercooling of -0.1°C or higher—an ice sheet forms over the water surface for lower rates of temperature change.

Wigle (1970) and Arden and Wigle (1972) describe a study in the Niagara River where frazil ice production began at a water temperature of -0.05°C during cold, clear nights, and developed into "a driving snowstorm such as can be seen through the headlight beams of a moving automobile at night." They estimated that the accumulated frazil ice reduced the cross-sectional areas of the river by as much as 25%. Experiments by Garabedian and Strickland-Constable (1974) shed light on the rapid multiplication of frazil ice nuclei through the mechanism of "collision breeding"; at a supercooling of -0.10°C, 44 crystals formed in 5 seconds from one original seed crystal.

Osterkamp (1978a) observed that the nucleation of frazil ice in rivers is heterogeneous for small values of temperature difference below the freezing point of water ΔT_n (or supercooling). In addition, he concluded that flow turbulence per se does not noticeably affect ΔT_n and that water of an ice-free river does not supercool to less than -0.05°C at depths of 10-mm and more below the water surface. In another paper, Osterkamp (1978b) reviewed various mechanisms for frazil ice nucleation and concluded that mass exchange and secondary nucleation are the most likely mechanisms. The former mechanism involves ice particles that originate at some distance from the water body (snow, frost, ice particles from banks, trees, etc.) and ice particles that originate in the river water; for example, water droplets or vapor can, on being propelled into the cold air above the water surface by splashing, wind spray and evaporation, freeze and fall back to the water surface after being spontaneously nucleated in the cold air.

Mueller (1978) conducted several experiments with temperatures of supercooling between -0.05° and -0.30°C in a turbulence jar (17.2 by 12 by 20 cm), which was an earlier version of the jar in which the present experiments were performed. Water in the jar was cooled below the freezing point by circulation of a coolant through tubes in the walls and base of the jar and turbulence was generated by a moving grid. In Mueller's experiments no frazil ice formed in the turbulence jar unless the supercooled water was seeded with ice nuclei. He found that this happened regardless of the degree of supercooling, the intensity of turbulence or the presence of foreign materials in the water.

In summary, the weight of both laboratory and field evidence strongly indicates that the heterogeneous nucleation of supercooled water by the ice fragments or crystals initiates the formation of frazil ice. Nevertheless, Hobbs (1974) alludes to the nucleation of supercooled water by the immersion of a cold metal rod in the water.

Particle size and evolution of frazil ice

Notwithstanding the many, although somewhat diffuse, descriptions of size and shape of frazil ice particles, the correlation of frazil ice geometry with water temperature has not been well delineated. In

addition, a rather varied terminology is used in published literature to describe frazil ice particles.

Field observations of frazil ice growth in rivers, as reported by Arakawa (1954), Michel (1967), Arden and Wigle (1972), Osterkamp (1978b) and others, indicate that frazil ice formation begins at a temperature of supercooling of the order of -0.05° to -0.1°C, with the frazil ice having the form of circular disks, 1 to 5 mm in diameter. Schaefer (1950) recorded the dimensions of frazil ice particles in the Mohawk River. He found that disk diameter ranged from 1 to 5 mm and disk thickness varied from 2.5×10^{-2} to 10^{-1} mm. Hobbs (1974) concluded that the circular disk is the preferred growth form for frazil ice forming in pure water that has been supercooled to within a temperature range of -0.1° to -0.3°C. The concensus of those who have observed frazil ice growth appears to confirm Hobbs' conclusion.

Laboratory experiments by Carstens (1966), Hobbs (1974), Mueller (1978) and other researchers report particle sizes for frazil ice ranging up to 10 mm in diameter. The larger sizes reported for frazil ice particles grown in laboratories are probably attributable to the lower water temperatures that can be attained, and used, in laboratory experiments. This observation, however, remains to be verified.

The evolution of frazil ice into larger agglomerates, according to Michel (1967, 1972) and Osterkamp (1978a), starts when crystals of 1 to 5 mm in diameter and 10^{-2} to 10^{-1} mm in thickness form "flocs" or collections of disks 5 to 100 mm in diameter; subsequently "pans" with diameters of the order of 1 m and thickness of 0.1 to 0.5 m form; "floes" with diameters of 1 to 30 m and thickness of 0.5 to 5 m may then form as patchworks of pans. Carstens' (1970) analysis of several Norwegian rivers showed that for surface velocity v_s greater than 0.6 m/s, but less than 1.2 m/s, frazil ice forms and accumulates on the water surface–for v_s greater than 1.2 m/s frazil ice forms over the whole river depth. These values are roughly in agreement with experiments conducted by Hanley and Michel (1977), who also found 0.24 m/s to be the threshold velocity for frazil ice formation.

Several anecdotal accounts of frazil ice accumulation in rivers and lakes have been published. A 16-km-long under-ice accumulation of frazil ice with an approximate volume of 5×10^7 m^3 in the La Grande River is described by Michel (1978). He observed that the accumulation began with the collection of frazil ice beneath the solid ice cover, which was some distance downstream from rapids. The open water at the rapids enabled the water to become supercooled. Beginning at a downstream location, the accumulation then progressed upstream. Michel (1978) and Tesaker (1975) developed a Froude number criterion to predict the maximum thickness of frazil deposition beneath the ice cover.

Influences of turbulence and water temperature on the rate of frazil ice formation

Although a number of analytical models of frazil ice growth have been formulated and several experimental studies of frazil ice growth conducted, no study has adequately explained the influence of turbulence and water temperature on the rate of frazil ice growth.

One of the earliest models of frazil ice growth was proposed by Carstens (1966), who suggested the following relationship for the rate of frazil ice growth, dM_i/dt (M_i = mass of ice, t = time):

$$\frac{dM_i}{dt} = \frac{1}{L_i}\left(S_H M_w \frac{dT}{dt} + Q_s\right) \qquad (1)$$

where L_i = latent heat of fusion
S_H = specific heat of water
T = water temperature
M_w = mass of water
Q_s = rate of heat loss from water surface.

Another expression for dM_i/dt, from the point of view of nucleation and growth of ice crystals, was proffered by Carstens for the rate of frazil ice production:

$$L_i \frac{dM_i}{dt} = \alpha A_t (T_m - T) \qquad (2)$$

where A_t = surface area of crystals at time t, T_m = freezing temperature of water, and α = heat transfer coefficient, given by

$$\alpha = \frac{k}{\ell} N_u \qquad (3)$$

where k = thermal conductivity of water, ℓ = characteristic dimension of ice crystals, and N_u = Nusselt number, which governs the heat transfer from ice surfaces. N_u depends on the geometry of ice crystals and on the structure of flow around the ice crystals. For a given geometry of ice crystal, Carstens proposed that

$$N_u = C_1 R_e^m \qquad (4)$$

where C_1 = constant
R_e = Reynolds number = $v\ell/\upsilon$

v = a characteristic velocity of the flow
υ = kinematic viscosity
m = constant (0.5 ~ 0.8).

Carstens further proposed that

$$A_t \sim N^{1/3} M_i^{2/3} \tag{5}$$

and

$$\ell \sim N^{-1/3} M_i^{1/3} \tag{6}$$

where N = number of ice crystals. By utilizing eq 3 through 6, we can rewrite eq 2 as

$$\frac{dM_i}{dt} \approx \frac{k}{L_i} M_i^{1/3} N^{2/3} R_e^m (T_m - T) . \tag{7}$$

Carstens concluded from observations of ice crystal formation in his experimental flume that the number of ice crystals N increases with increasing rate of heat loss Q_s. This observation was in agreement with his analytical formulation, expressed in eq 1 through 7. An important observation indicated by his experimental and analytical data is that, for decreasing values of the Reynolds number, the required condition for prolonged periods of supercooling can be determined from the relationship

$$R_e^m N^{2/3} M_i^{1/3} = \text{constant}. \tag{8}$$

In addition to formulating the above analytical model of frazil ice formation, Carstens also conducted experiments in a race-track shaped flume (1.2 by 0.3 m by 0.2 m wide) at the Technical University of Norway. The bottom and sides of the flume were insulated, thereby allowing heat loss only through the free surface to the air stream above. The air temperature was maintained at -10°C. With a cooling rate of 0.01°C/minute, he attained a maximum supercooling of -0.04°C. The rate of cooling was varied by changing the temperature and the distance between the flume and a fan that controlled air speed. His experimental results show that an increase in the rate of heat loss increased the temperature of supercooling attained, the residual supercooling temperature and the rate of temperature rise from maximum supercooling.

The results of Mueller's (1978) experiments show that the growth rates of frazil ice particles increase with greater supercooling and higher grid velocity (that is, with increased turbulence). From his observations that the heat transfer per particle could be normalized with supercooling and that the size of particles was constant in all experiments, Mueller concluded that the rate and the total amount of frazil ice production can be predicted if estimates of the number of particles and heat transfer per particle can be made. He suggested that the normalized heat transfer can be related to the turbulent characteristic of flow, but a nucleation theory was not available to estimate the number and growth rate of frazil particles. His experiments also indicated that frazil production increases with increasing grid frequency or level of turbulence intensity.

Andres (1982) carried out an experimental program to study the effects of turbulence and the rate of heat loss on the supercooling of water and the subsequent frazil ice formation. He performed his experiments using an octagonal tank at the base of which was mounted a propeller to generate a cyclostrophic flow in which the frazil ice formed. From his data, Andres observed a trend that indicated that, for increasing values of turbulence intensity, the period of supercooling decreased but the rate of frazil ice formation increased. The roles played by turbulence and water temperature in the rate of frazil ice formation are difficult to define from Andres' data.

An elaborate mathematical model of frazil ice formation and transport in a river with a steady flow was constructed by Matousek (1981). His model is formulated using a heat balance equation for a steady uniform flow. In his state-of-the-art review of research concerning frazil ice, Tsang (1982) derived the following relationship for the rate of ice production:

$$\frac{\partial c_i}{\partial t} = \frac{S_H}{L_i} \frac{\partial T}{\partial t} + \frac{Q_s - Q_i}{\rho L_i D} \tag{9}$$

where c_i = concentration of frazil by weight
S_H = specific heat of water
T = water temperature
L_i = latent heat of fusion of ice
Q_s = heat flux from water to air
Q_i = heat flux from channel bed to water
D = flow depth.

By noting that $\partial c_i/\partial t = 0$ just prior to nucleation, we may rewrite eq 9 as

$$\frac{\partial c_i}{\partial t} = \frac{S_H}{L_i} \left[\frac{\partial T}{\partial t} - \left(\frac{\partial T}{\partial t}\right)_n\right] \tag{10}$$

where $(\partial T/\partial t)_n = \partial T/\partial t$ at nucleation. Integration of eq 10 yields

$$c_i = \frac{S_H}{L_i}(T - T_o) - \frac{S_H}{L_i}\left(\frac{\partial T}{\partial t}\right)_n (t - t_n) \qquad (11)$$

where T_n = nucleation temperature and t_n = the time of first nucleation. Tsang comments that, as seen from eq 11, frazil concentration (c_i) is greatly influenced by $(\partial T/\partial t)_n$ which, in turn, is determined by heat fluxes to and from the water body.

Analytical models such as those constructed by Carstens (1966), Matousek (1981) and Tsang (1982) are useful in that they may indicate the nature of frazil ice formation and its relationship with water temperature and turbulence. However, a drawback of these models is that they are rather unwieldy and difficult to use.

Conclusions

Despite the burgeoning amount of work that has been invested in the study of frazil ice, the three issues outlined in the *Scope of Study* section have remained largely unaddressed. These are the influences of both water temperature at nucleation and turbulence characteristics of a flow on the rate of frazil ice formation and the variation of frazil ice particle size with the temperature and turbulence of a flow.

Evidence from reported observations suggests that natural rivers and streams rarely become supercooled to temperatures less than about -0.1°C. Frazil ice particles formed at this temperature tend to be disks with diameters typically attaining a maximum value of approximately 2 to 3 mm, and thicknesses varying from 10^{-2} to 10^{-1} mm. Larger diameters of frazil ice particles are reported from laboratory studies, frequently involving lower water temperatures than are recorded for rivers and streams, thus suggesting that particle size is a function of water temperature. The influence of turbulence on particle size appears not to have been studied. The amount, or concentration, of frazil ice that forms in a flow is indicated by several researchers to increase with turbulence intensity of a flow, but it is unclear if this occurs by turbulence causing the water to become supercooled to lower temperatures as well as by playing a direct role in the physics of frazil ice formation. Field data (for example those reported by Tsang [1982]) indicate that an upper limit to the concentration of frazil ice that can be formed in supercooled water of streams, rivers and lakes is of the order of 0.5% by weight.

ANALYTICAL MODEL

Introduction

By combining elements of heat transfer theory associated with the formation of ice in liquid water with elements of turbulence theory, as it applies in a turbulence jar, it is possible to identify the influences of water temperature and turbulence on the rate of frazil ice formation. Experimentation was used to gain knowledge of the influences of turbulence and water temperature on the temporal variation of frazil ice particle size. Turbulence was generated in the turbulence jar by a vertically oscillating grid that had to be heated to stop frazil ice from adhering to it.

The analytical model is developed from a Lagrangian standpoint—that is, the formation of frazil ice is considered for a supercooled parcel or volume of water moving with the flow in a stream, river or lake. The analysis deals with the rates and the amounts of frazil ice that can form in a parcel of water that has been supercooled to a temperature T_o prior to the formation of frazil ice.

Elements of heat transfer

When ice is formed in supercooled water, latent heat of fusion is released, thereby raising the temperature of the surrounding water. The rate of frazil ice formation can be related to the rate of latent heat release in order to provide a framework for the study of the influences of water temperature and turbulence on the rate of frazil ice formation. Formulation of the analytical framework proceeds as follows. The rate at which heat is taken up by the water is given by

$$Q_w = \rho S_H V \frac{d}{dt}(T - T_m) \qquad (12)$$

where ρ = water density
S_H = specific heat of water
V = volume of water
T = water temperature
T_m = equilibrium temperature of liquid water and ice (for pure water, T_m = 0°C).

The rate at which heat is transferred to the water from its surroundings and from the heated agitator grid is

$$Q_h = \rho S_H V \dot{T} \qquad (13)$$

where $\dot{T}$ = the rate of temperature rise attributable to these heat sources. It was experimentally found that $\dot{T}$ could be taken to be constant for a given combination of ambient air temperature and grid temperature. The temperature rise terms are illustrated in Figure 2.

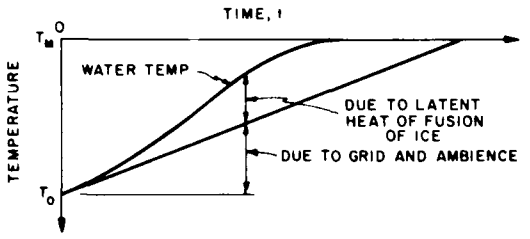

Figure 2. Temporal variation of temperature in the turbulence jar (T_o = water temperature at seeding).

The surface area of frazil ice crystals, A_t, at any time t after seeding can be expressed as

$$A_t = A_o + \frac{\rho S_H V}{\rho_i L_i \ell} (T - T_o - \dot{T}t) \qquad (14)$$

where A_o = surface area of ice at $t = 0$ (the time of seeding)
ρ_i = density of ice
L_i = latent heat of fusion of ice
ℓ = characteristic thickness scale of the ice particles
T_o = supercooling at the time of seeding.

As frazil ice particles are flat platelets, the surface area of ice need not be reckoned in terms of particle shape and number of particles. Rather, the particles can be considered to be fragments of a single, thin ice sheet, with heat being transfered from both faces of the sheet. Heat transfer from the edges of the sheet can be neglected. The surface area in eq 14 represents the area of both faces of the ice sheet. The rate at which heat of fusion is given up by the ice particles is

$$Q_f = \alpha[A_o + \frac{\rho S_H V}{\rho_i L_i \ell} (T - T_o - \dot{T}t)] (T_m - T) \qquad (15)$$

where α = coefficient of heat transfer between the frazil particles and water.

Equating Q_w to the sum of Q_h and Q_f yields

$$\frac{dx}{dt} = \dot{T} - (Bt + A) x - Cx^2 \qquad (16)$$

where $x = (T - T_m)$, and

$$A = \frac{\alpha}{\rho S_H V}\left[A_o + \frac{\rho S_H V}{\rho_i L_i \ell} (T_m - T_o)\right]$$

$$B = \frac{\alpha \dot{T}}{\rho_i L_i \ell}\ ;\ C = \frac{\alpha}{\rho_i L_i \ell}\ .$$

For pure water and the Celsius temperature scale ($T_m = 0$), $x = T$, and thus eq 16 becomes

$$\frac{dT}{dt} = \dot{T} - (Bt + A) T - CT^2\ . \qquad (17)$$

If the surface area of the edges of a frazil ice platelet (the platelets typically are about 0.05 to 0.10 mm thick) is neglected, the characteristic width ℓ can be taken to be $b/2$ and the frazil ice concentration at time t, c_t, is expressed as

$$c_t = \frac{A_t b}{2V} = \frac{A_o b}{2V} + \frac{\rho S_H}{\rho_i L_i} (T - T_o - \dot{T}t) \qquad (18)$$

where b = representative thickness of frazil ice platelets, which was assumed to remain constant at a value of 0.1 mm throughout each experiment.

Note that T can be removed from eq 17 and 18 to yield a differential equation for frazil ice concentration c_t. It is clear, both from physical reasoning and eq 18, that c_t varies linearly with $(T - T_o - \dot{T}t)$, or if T and $\dot{T}$ are both set to zero, c_t varies linearly with temperature of supercooling T_o.

Several refinements to the above analysis can be considered. One refinement is to allow the heat transfer coefficient α to decrease with increasing concentration of frazil ice. As the concentration of frazil ice increases, the effective dynamic viscosity of the water-ice mixture increases because the supercooled water that was initially clear ultimately becomes a slush. The following heuristic relationship was formulated to describe the variation of α with the concentration of frazil ice c_t:

$$\alpha = \alpha_o n_1 (1 + n_2 e^{-(n_3 c_t)}) \qquad (19)$$

where α_o = initial value assumed for the heat transfer coefficient when concentration c_t is zero, and n_1, n_2 and n_3 are experimentally determined constants.

Equation 17 was solved for several values of α_o in order to give the temporal values of mean water temperature and concentration of frazil ice for supercooled water. To facilitate the solution, A_o

was assumed to be equivalent to a single frazil ice crystal with two 0.25-cm^2 surfaces and a thickness of 0.1 mm. This is typical of the size of frazil ice particles that were observed during the experiments, and gives a volume equivalent to the piece of seeding ice. Results were produced from the analytical model by way of a computer-based Runge-Kutta solution routine, with the Gill modification. A listing of the computer program used to facilitate the solution is given in Appendix B.

The foregoing analysis, eq 12 through 19, is a global description of frazil ice formation in a parcel of supercooled water. It does not account for the influences of the temporal variation of size and size distribution of frazil ice on the rate and amount of it formed in a parcel of supercooled water. Additional limitations of the analysis include the lack of detailed relationships among the growth of frazil ice crystals, secondary nucleation and heat transfer from suspended crystals in a turbulent fluid. Nonetheless, the analysis elucidates the roles played by water temperature and turbulence level on the rate and amount of frazil ice formed in a body of supercooled water. It also provides a suitable framework into which further analytical refinements can be added.

Elements of turbulence

The relationships between the turbulence structure of a flow and the formation of frazil ice or, more pertinently, between turbulence and heat transfer from a frazil ice particle, are involute and not well defined. Essentially, the action of turbulence is to increase the rate of heat transfer from frazil ice particles and thereby to increase the rate of frazil ice formation. This happens provided that the particles are considerably larger than the Kolmogorov length scale or microscale of the turbulence field in which they form, and that the frazil ice particles are well spaced, so that they can be treated as single particles in a shear flow.

The heat transfer from small ice particles to their surrounding fluid depends on the ratio of the microscale of turbulence to the size of the particle. Ice particles are convected with the fluid without sensing turbulence if the microscale is large compared to the particle. Consequently, the relative motion and the heat transfer between the particle and fluid are small. As the ratio of turbulence microscale to particle size decreases, the rates of relative motion and heat transfer increase. In addition, as long as the level of turbulence is such that the microscale for time is short compared to the time scale of heat conduction, the heat transfer from a frazil ice particle to the fluid will be an order of magnitude higher than if the fluid were at rest. The relative magnitudes of convective heat transfer and heat transfer by conduction are usually expressed in terms of the Nusselt number N_u,

$$N_u = \frac{\alpha L}{k} \tag{20}$$

where k = coefficient of thermal conductivity and L = a characteristic length. Nusselt numbers are frequently related to Reynolds and Prandtl numbers, R_e and P_r, respectively; for example

$$N_u = K R_e^n P_r^m$$

$$\left(\frac{\alpha L}{k}\right) = K \left(\frac{vL}{\upsilon}\right)^n \left(\frac{S_H \upsilon \rho}{k}\right)^m \tag{21}$$

where n and m = exponents
K = constant
S_H = specific heat of the fluid
υ = kinematic viscosity of the fluid
ρ = density of the fluid.

Equation 21 is primarily used to evaluate the heat transfer coefficient α for a particular flow case. Carstens (1966) and Mueller (1978) adopted lines of analysis involving eq 21 in order to estimate the rate of heat transfer, and thus the rate of frazil ice formation, for various levels of turbulence in a turbulence jar. Because of the lack of a well-developed theory to describe the motion of, and heat transfer from, discoidal particles in a shear flow, the lines of analysis involving relationships of the form of eq 21 as followed both Carstens and by Mueller are fraught with many difficulties.

The approach followed in the analysis conducted for this study was to use the principles of particle suspension in a turbulent flow to obtain estimates of turbulence level, then to obtain values of heat transfer coefficient α by calibrating the analytical model of frazil ice formation with the experimentally determined values of turbulence exchange coefficient ϵ.

Drawing on an analogy with Prandtl's mixing-length theory (1925) for turbulence, Rouse (1937) described the suspension of particles in a flow in the following manner: "If at any flow depth there are n particles per unit volume of fluid, the concentration gradient being written [as] dn/dy, then due to transverse fluctuations, fluid masses bearing n particles per unit volume will be carried a mean distance [ℓ_p Prandtl mixing length] across the flow to regions where the concentration differs by the amount [$\ell_p\, dn/dy$]. Thus, the temporal rate of passage of

sediment per unit area [N_s] will be the product of the rate per unit area of transverse flow [$|v'y|$] and the difference between the sediment concentration in the traveling fluid mass and that of the region into which it comes [$-\varrho_p\, dn/dy$]." Rouse wrote

$$N_s = |v'y|\,\varrho_p \frac{dn}{dy} \quad . \tag{22}$$

The variation of suspended particle concentration with depth can be related to the turbulence characteristics of the flow by using the following relationships proposed by Rouse (1938): "For sediment suspension it is customary to assume that a state of equilibrium [exists] between the mean vertical rate of sediment transport due to turbulence and the normal rate of settling of sediment due to its own weight. Thus, if w denotes the settling velocity [of the suspended particles] and [c_s] is the sediment concentration per unit volume of the suspension

$$c_s w = -\beta\, v'\, \varrho_p \frac{dc_s}{dy} \quad . \tag{23}$$

Integration leads at once to an expression for the relative concentration [of suspended particles] at any point above some arbitrary reference level a,

$$\ln\left(\frac{c_s}{c_{sa}}\right) = -\frac{w}{\beta} \int_a^y \frac{dy}{v'\varrho_p} \tag{24}$$

the magnitude of [c_{sa}] depending ultimately upon conditions in the boundary region." In the foregoing quotations, the bracketed portions and the equation numbers are inserted by the authors. It is pertinent to note in Rouse's analysis of particle suspension by turbulence that the turbulence momentum exchange coefficient ϵ is equated to $\beta\epsilon_s$, where ϵ_s is the turbulence mass transfer coefficient and β is a proportionality coefficient, which for fine sediments (fine sands and silts) is assumed to be of the order of unity. For coarser sediments β may decrease with increasing particle size and no longer be a constant value, although this is still a matter of some controversy.

The turbulence jar, being a tank in which a grid oscillates with simple harmonic motion, produces a flow with essentially the same degree of mixing ($v'\varrho_p$) that is constant over the major portion of the fluid volume. The turbulence jar is, therefore, well suited for the study of heat transfer and frazil ice formation in a turbulent flow. Integration of eq 24 for constant $v'\varrho_p$ yields

$$\frac{c_s}{c_{sa}} = e^{-\frac{w}{\epsilon}(y-a)} \tag{25}$$

in which the turbulence exchange coefficient ϵ is equated to $\beta\, v'\varrho_p$. Rearranging eq 25 leads to

$$\frac{(y-a)}{\log\left(\frac{c_{sa}}{c_s}\right)} = 2.3\,\frac{\epsilon}{w} \tag{26}$$

from whence, noting that the left-hand side of eq 26 is equal to the slope of the concentration versus depth curve S,

$$\epsilon = \beta\, v'\varrho_p = \frac{Sw}{2.3} \quad . \tag{27}$$

By measuring the distribution of suspended sediment concentration over the depth of the turbulence jar, it is possible to relate the characteristic magnitude of the turbulence exchange coefficient ϵ to the frequency of grid oscillation F_g. A relation between ϵ and F_g is developed from experimental results in the *Results* section.

EXPERIMENTATION

Experimental apparatus

Several designs of experimental apparatus to produce a turbulent flow field were investigated during the course of the study. The experience gained from using various flow devices to produce a turbulence field for study of the effect of turbulence and water temperature on frazil ice formation led to the formulation of the following guidelines for experiments of this kind:

1. Every nonstationary boundary, be it an agitating grid, propeller or moving walls of a container, must be heated to a sufficiently high temperature so that frazil ice does not adhere to it (or otherwise made ice-phobic). Otherwise, frazil ice will accumulate on the moving boundary, which can then sweep it through the fluid and lead to high rates of ice nuclei formation and frazil ice dispersion that would be artifacts of the particular apparatus.

2. The primary fluid motion must persist for several minutes without external influences. This period is required for the growth of the initial ice nuclei or crystals, the transfer of heat from them, their rupture, their dispersion and the formation of frazil ice flocs until the sensible heat associated with

latent heat of fusion accompanying ice growth is absorbed by the supercooling. This consideration precludes the use of relatively short recirculating flumes for many types of frazil ice experiments, because the agitation and attendant frazil ice formation that may take place in the pump and during flow passage through the return pipe completely dominates the frazil ice formation that takes place in the working section of the flume.

3. The apparatus must permit easy control of the temperature or degree of supercooling of the water.

4. The apparatus must be constructed so that a controllable quantity of seed crystals for frazil ice nucleation can be easily introduced into the supercooled water.

5. The water being used in the experiments must be shielded from intrusion of ice crystals from the air or other sources.

A turbulence jar was found to be best suited to the present experiments, which used a turbulence jar similar to that described by Mueller (1978) and Mueller and Calkins (1978). However, the jar was modified so that the supercooled volume of water could be isolated from the chilling elements that cooled the water. The turbulence jar is shown in Figures 3 and 4. Figure 3 shows the experimental setup, while Figure 4 is a closeup of the turbulence jar. Dimensions of the jar are given in Figure 5. The metal sidewall and bottom panels of Mueller's turbulence jar, which were used for chilling the water,

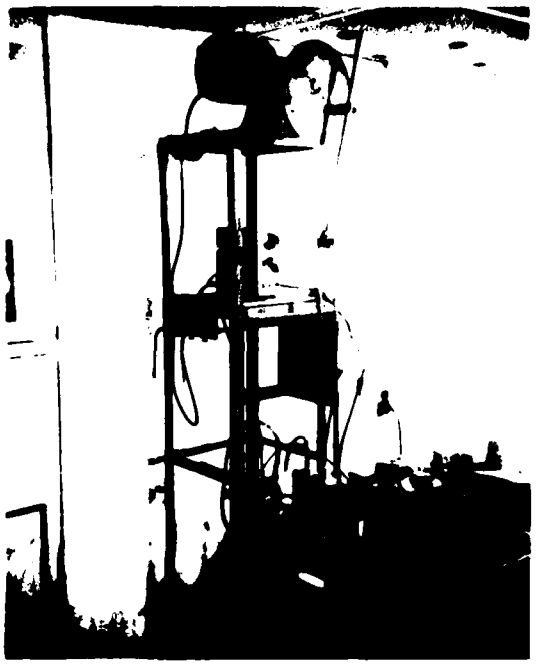

Figure 3. Experimental apparatus.

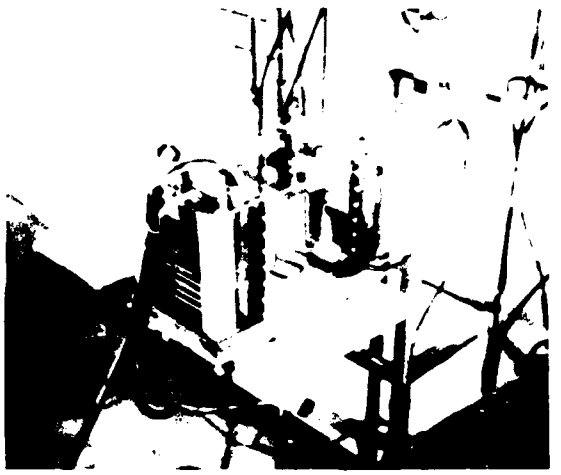

Figure 4. Turbulence jar.

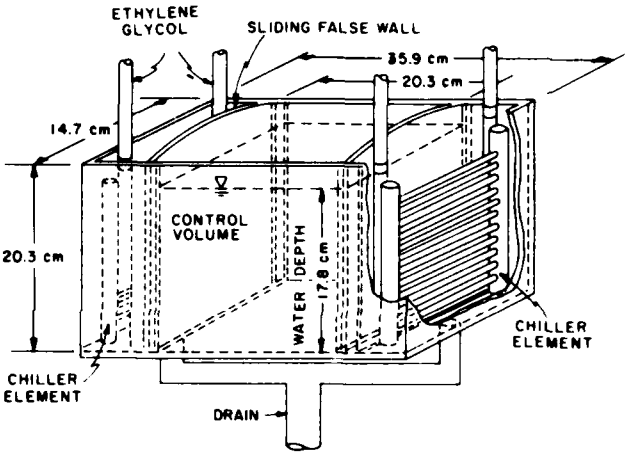

Figure 5. Dimensions of the turbulence jar.

frequently became covered by a layer of boundary-fast ice. Ice that freezes to the jar boundaries is lost from the frazil ice field, reducing the number of nucleation centers present in the liquid water and thereby affecting the experimental results. For the modified turbulence jar, once the desired temperature of supercooling was attained, the central water compartment was isolated from the two chiller elements. The side compartments containing the chiller elements were then drained to further isolate the chiller elements from the test compartment.

The water in the turbulence jar was supercooled by circulating a chilled ethylene glycol solution through two chiller elements. The ethylene glycol solution was maintained at a temperature of -2°C. An oscillating grid attached to a scotch yoke (see Fig. 3) was used to agitate the water in the jar. The grid was made of 6-mm-diameter tubing that was

bent into loops spaced 30 mm apart (see Fig. 4). During the phase of each experiment in which frazil ice was being formed, the grid was heated in order to stop the frazil ice from adhering to it.

Early tests were conducted with an unheated grid, but these tests proved to be unsuccessful because, within a short time after seeding, the frazil ice adhered to the grid. Thereafter, as the grid oscillated, it moved the frazil ice conglomeration adhering to it through the water and in the process accumulated more frazil. Consequently, the mechanisms of interest–frazil ice crystal dispersion and frazil ice floc and particle rupture by turbulence–were no longer the dominant mechanisms in the experiments; turbulent diffusion was insignificant compared to frazil advection by the moving grid. Moreover, the turbulence produced by the grid motion changed as ice accumulated on the grid and altered its effective dimensions.

The rise of water temperature because of heat input from the heated grid and from the air surrounding the turbulence jar provided a "base-line" of temperature rise with time, as is shown in Figure 2; temperature rise above this line is ascribable to latent heat release during the formation of frazil ice. During the experiments, air temperature around the jar was kept at about 1° to 2°C.

Much effort was devoted to perfecting the experiments. Yet, although many of the difficulties involved in conducting frazil ice experiments were overcome, several problems could not be readily solved or circumvented. Some preliminary experiments were also conducted in the refrigerated flume operated by the IIHR and in a couette-flow annulus. However, both of these apparatus were found not suitable for studying the influences of water temperature and turbulence on frazil ice formation. The conclusions derived from the use of the flume and the couette-flow annulus are briefly discussed in Appendix A.

Experimental procedure

During each experiment, the deionized water contained in the turbulence jar was supercooled using the two chiller elements depicted in Figure 5. In order to prevent an illegitimate nucleation of the water by extraneous ice crystals introduced from the air surrounding the turbulence jar, the air temperature in the ice room was maintained at 1° to 2°C. Water temperature in the turbulence jar was registered by means of a fast-response thermistor probe. The probe was positioned so as to protrude horizontally about 20 mm from one sidewall into the water at its mid-depth. The probe's tip had to extend at least 7 mm from the sidewall to be sufficiently outside a thin temperature boundary layer at the walls of the turbulence jar.

When the water in the turbulence jar had been cooled to a temperature just below the desired temperature of supercooling, the central control volume was isolated from the chiller grids by the insertion of the two sliding sidewalls. At the same time, the heating element of the agitator grid was activated. On attaining the specified temperature of supercooling, a small piece of ice, having a volume of approximately 0.025 cm^3, was dropped into the water. After a period of about 5 to 10 seconds, depending on the temperature of supercooling and the frequency of grid oscillation, frazil ice crystals became visable. The temperature of the water and ice mixture was recorded continuously, using a Gould strip-chart recorder, until the temperature slightly exceeded 0°C. The temperatures of supercooling T_o and frequencies of grid oscillation F_g that were used in the study are listed in Table 1. Several tests were conducted for each combination of T_o and F_g.

A series of tests was conducted to measure the growth rate of frazil ice particles with time for various values of T_o, F_g and ϵ. The frazil ice particles were removed from the turbulence jar by means of a fine-mesh net fixed to the end of a spatula. The spatula was chilled to just below 0°C prior to its immersion into the turbulence jar. The spatula with frazil ice particles, on removal from the jar, was placed in a freezer box. A six-power optical comparator with a reticle graduated into 0.1-mm increments was used to measure the size of the frazil ice particles.

Table 1. Program of experiments.

Initial supercooling temperature (°C)	*Grid oscillation (cycles/min.)*
-0.05	15,30,60,75,100
-0.10	15,30,60,75,100
-0.25	15,30,60,75,100
-0.55	15,30,45,60,75,100
-0.60	15,30,45,60,100
-0.70	15,30,45,60,100
-0.90	15,30,45,60,75,100

Values of the turbulence exchange coefficient ϵ for the agitated water in the turbulence jar were determined by measuring the vertical distribution of suspended sediment concentration in the turbulence jar. A 20-mm-thick layer of 0.1-mm-diameter sand was placed over the base of the jar; the action of the oscillating grid caused some of the sediment to become suspended throughout the depth of the turbulence jar. Concentrations of suspended sediment were determined by withdrawing a volume of water and sediment at several elevations in the jar. A

narrow-nozzle pipette, with a capacity of 10 cm^3, was used to extract the sample volumes of sediment-bearing water. The sediment contained in each sample was then weighed. The weight of sediment in a sample with a low sediment concentration was determined by carefully sluicing the sediment onto a flat-bottomed dish and then estimating, with the aid of the optical comparator, its volume and then calculating its weight. The weights of sediment in the samples with higher sediment concentrations were determined by direct weighing. The weight concentrations of the samples were estimated from the weights of sediments contained in the sample volumes.

RESULTS

Introduction

Records of the temporal rise of water temperature for the experiments involving the combinations of initial temperature of supercooling and frequency of grid oscillation listed in Table 1 are presented. The temporal records of water temperature rise as determined using the analytical model are given in Appendix C. The rise in water temperature is proportional both to the amount of frazil ice formed in the turbulence jar and to the heat input from the oscillating heated grid. The experimental data were used to calibrate the analytical model, which was used to determine the rate of frazil ice formation as a function of water temperature and turbulence.

Nucleation of frazil ice

Various methods for seeding the supercooled water in the turbulence jar were tested. The two principal methods that were used involved either withdrawing a specified volume (usually about 20 cm^3) using a syringe, exposing it to an ice crystal, then injecting the fluid plus ice nuclei back into the turbulence jar, or dropping a "standard" piece of ice (about 0.025 cm^2 in volume) into the turbulence jar.

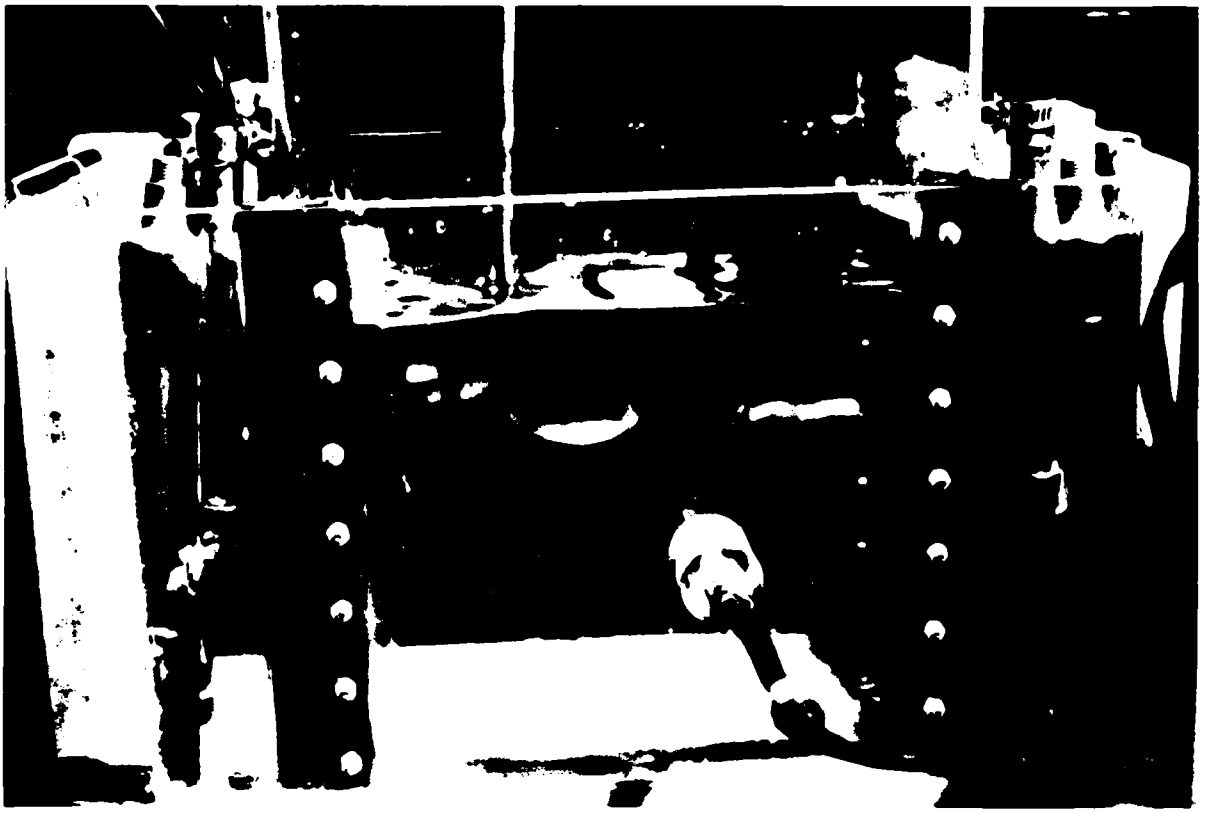

a. $t < 0^\circ$, *water undergoing supercooling.*

Figure 6. Frazil ice formation in the turbulence jar ($T_o = -0.55^\circ C$, F_g = *75 cycles/minute).*

For each method there was no difference in the manner of frazil ice formation, provided that the water and ice in the syringe were not vigorously agitated; when this happened, a larger amount of frazil ice nuclei could be introduced into the turbulence jar and thus lead to a slightly greater rate of frazil ice formation. For most of the experiments, the turbulence jar was initially seeded by dropping in a standard piece of ice.

As in the experimental studies by Mueller (1978) and others, as well as in the field observations reported by Osterkamp (1978b), this study found that there was no spontaneous or homogeneous nucleation of the supercooled water. In all experiments, seeding was required to initiate frazil ice formation. The formation of frazil ice in the turbulence jar is illustrated in the series of photographs presented in Figure 6. Figure 6a depicts the water being cooled to a temperature of -0.55°C at a frequency of grid oscillation of 75 cycles/min. Small disks of frazil ice are forming in the supercooled water, 20 seconds after nucleation (Fig. 6b). Some 50 to 70 seconds after nucleation (Fig. 6c and d respectively), the frazil ice particles have increased in size to a mean diameter of about 6 to 7 mm.

Subsequent to the seeding of the water, a brief period, typically 5 to 10 seconds, elapsed before frazil ice particles appeared in the turbulence jar. Once a few frazil ice ice particles had appeared, the particles multiplied rapidly. The rapid increase in the number of frazil ice particles formed can be ascribed to the process of collision breeding; frazil ice particles, by colliding with the solid boundaries of the turbulence jar, the oscillating grid or with each other, produce an increasing number of ice nuclei.

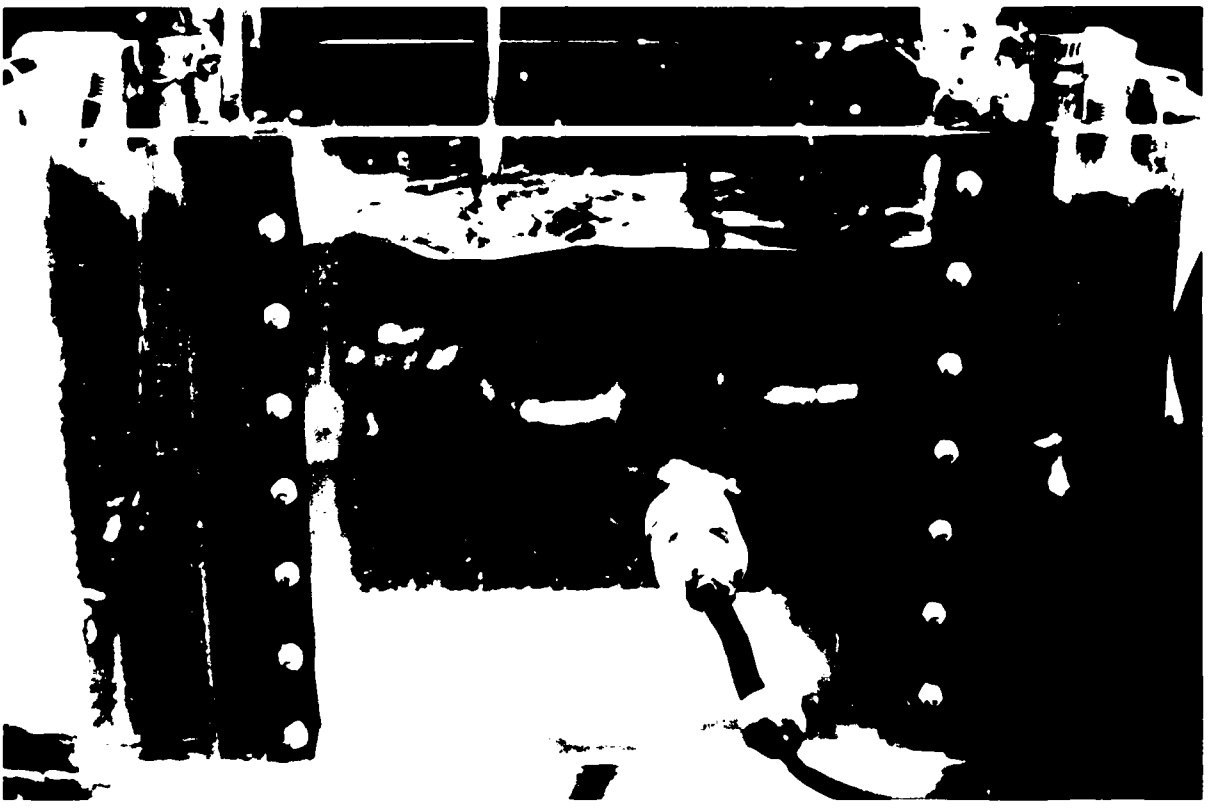

b. t = *20 seconds,* T = *-0.47°C.*

Figure 6 (cont'd).

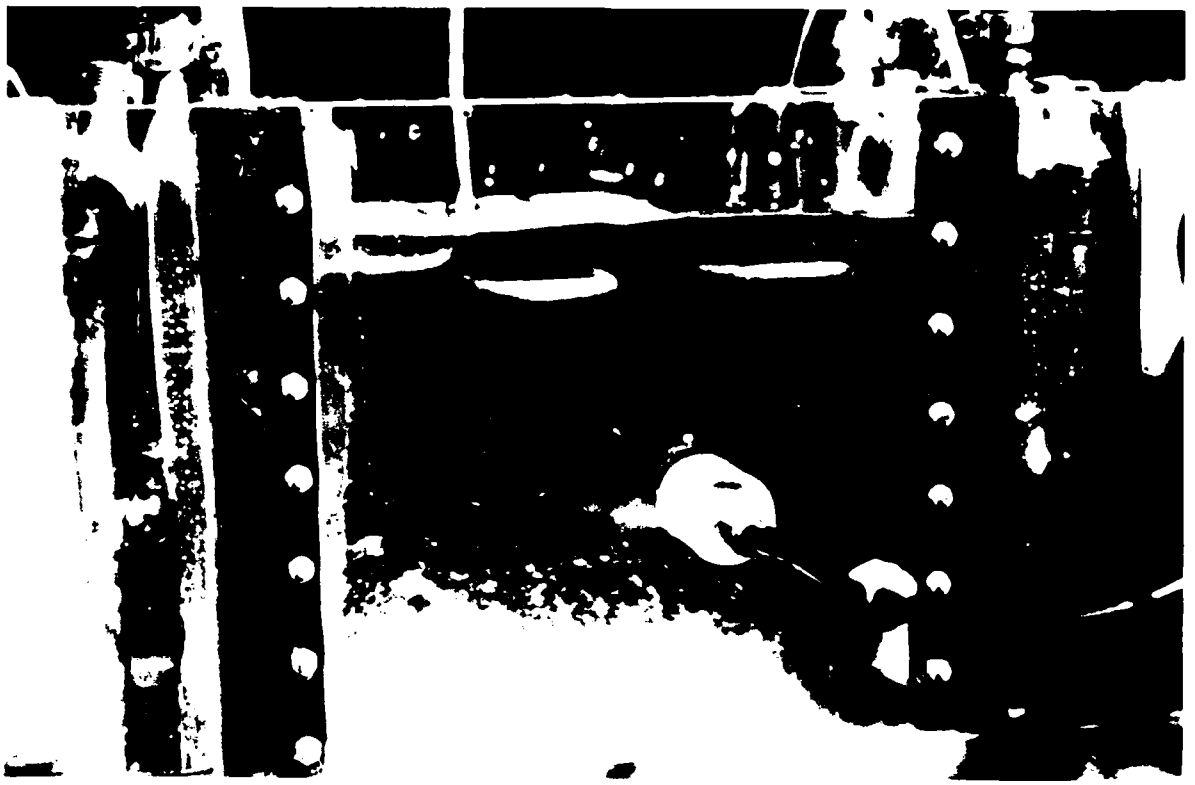

c. t = *50 seconds,* T = *-0.19°C.*

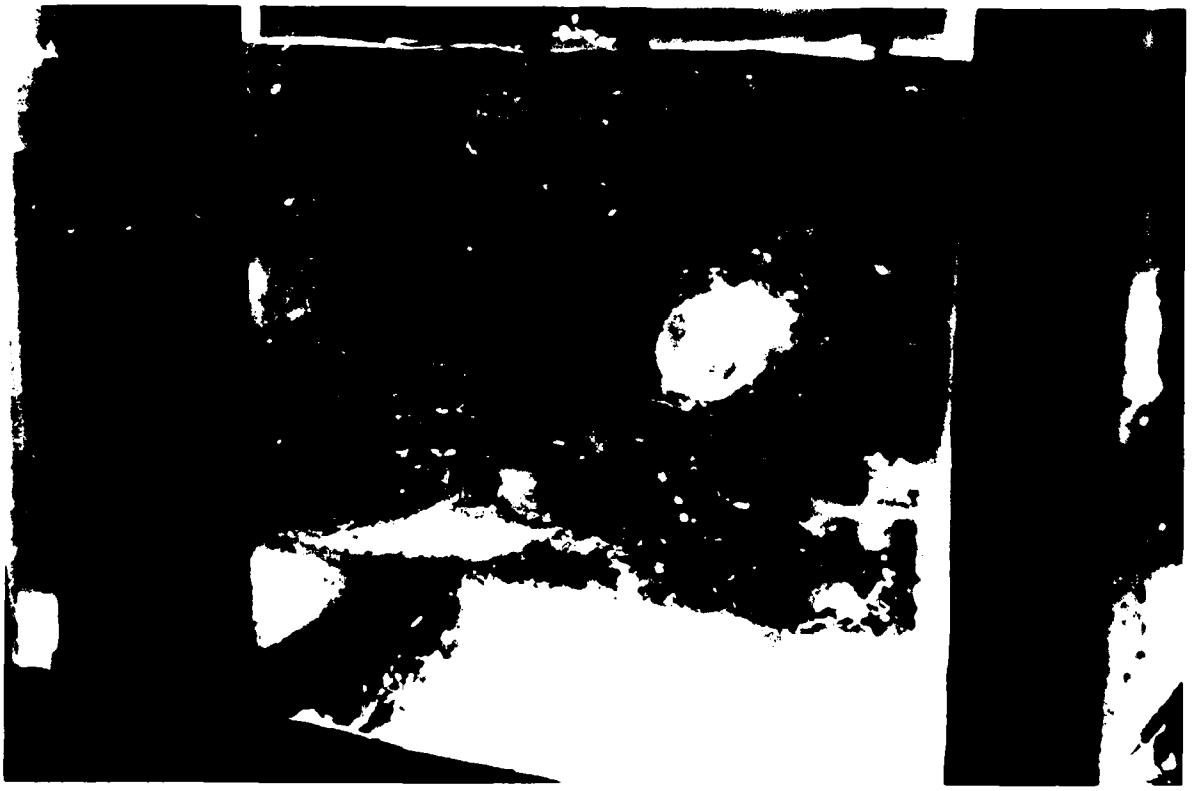

d. t = *70 seconds,* T = *-0.05°C.*

Figure 6 (cont'd). Frazil ice formation in the turbulence jar (T_o = *-0.55°C,* F_g = *75 cycles/minute).*

Influences of turbulence on frazil ice formation

As the turbulence intensity of a flow increases, the rate of frazil ice formation increases. The increase in the rate of frazil ice formation is primarily caused by both the increased rate of heat transfer between the frazil ice particles and the surrounding water and an increased rate of floc rupture, which provides more ice nuclei. As shown by the experimental data, the influence of turbulence on the rate of frazil ice formation appears to be more pronounced for lower temperatures of supercooling. This result can be observed from the records of experimental data that are presented in Figure 7.

The solid line curves in Figure 7 were fitted to temperature measurements that were recorded for several experiments at constant values of T_o and frequency of grid oscillation. The dash-dot curves are plotted in order to indicate the range of the experimental data. Although the trends for temperature rise—that is, frazil ice formation—indicate that the rate of frazil ice formation generally increases with greater values of grid oscillation frequency, a clear trend is not always apparent, especially for values of T_o equal to -0.10°C and -0.05°C.

It would appear from the experimental data that the rate of frazil ice formation may not be quite as

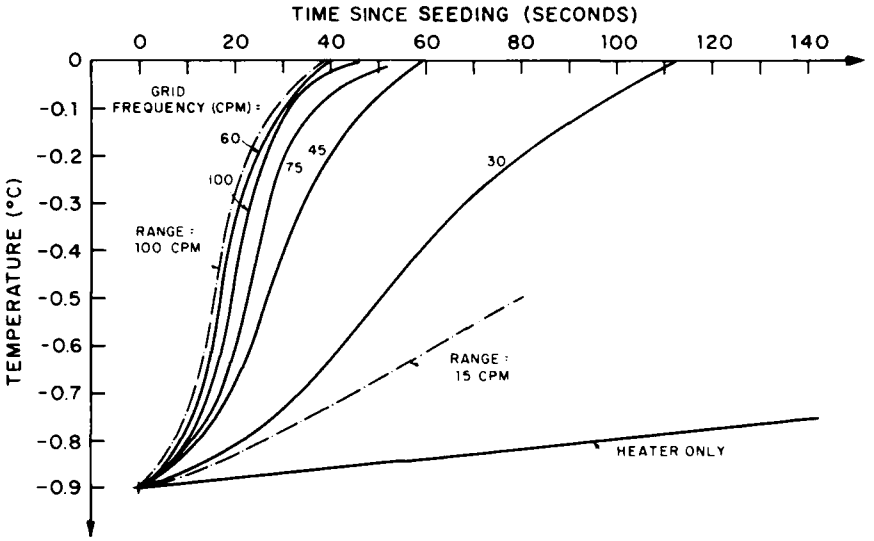

a. $T_o = -0.90°C$.

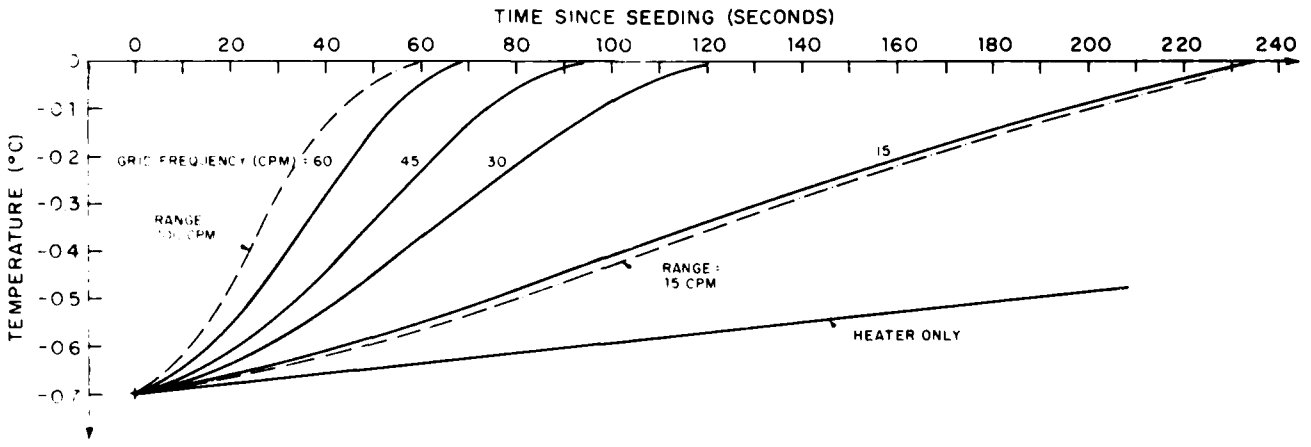

b. $T_o = -0.70°C$.

Figure 7. Experimental data. The solid curves are plotted for the mean results for each grid frequency, and the dash-dot lines indicate the range of the data (CPM–cycles per minute).

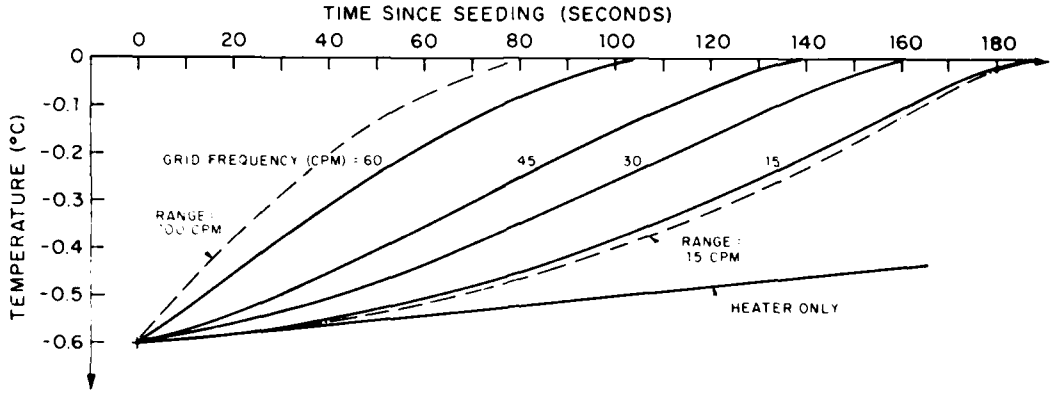

c. $T_o = -0.60°C$.

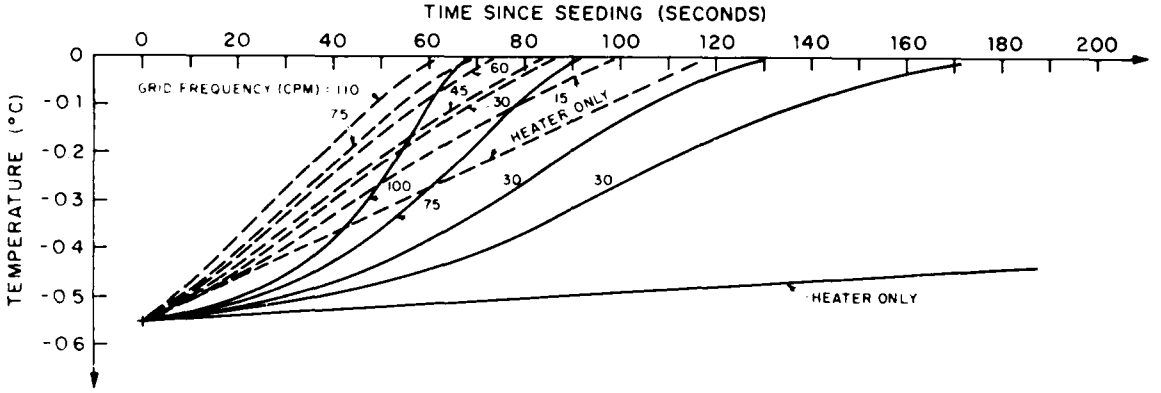

d. $T_o = -0.55°C$ *(two heater settings).*

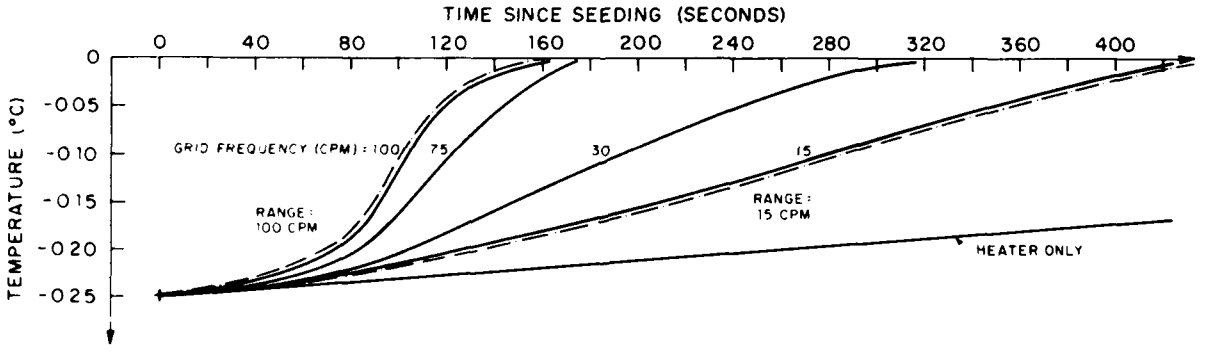

e. $T_o = -0.25°C$.

Figure 7 (cont'd). Experimental data. The solid curves are plotted for the mean results for each grid frequency, and the dash-dot lines indicate the range of the data (CPM–cycles per minute).

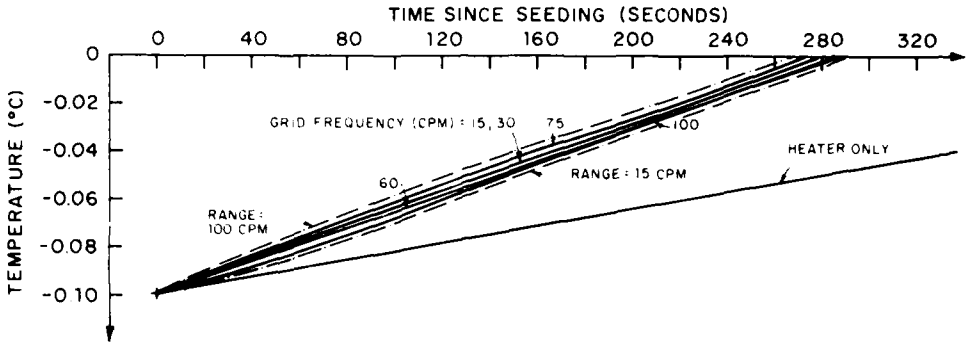

f. $T_o = -0.10°C$.

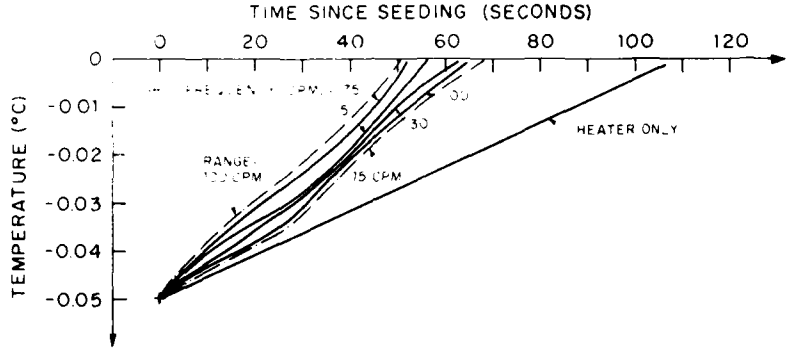

g. $T_o = -0.05°C$.

Figure 7 (cont'd).

sensitive to turbulence intensity as has been suggested in recent literature (Mueller 1978, Mueller and Calkins 1978, Martin 1981). Rather, turbulence intensity may indirectly exert a greater influence on the rate and quantity of frazil ice formation by influencing the temperature to which a body of water can be supercooled. When T_o is equal to either -0.10°C or -0.05°C, the relationship between the rate of temperature rise and frequency of grid oscillation appears to weaken. In both Figures 7f and g, bands enclosing the experimental data are shown and the overlap of some of the temperature-time curves is indicated. Although the rate of frazil ice formation increases slightly with increased level of turbulence, the trend is not sufficiently marked that the vagaries of experimentation cannot mask it.

The rates of frazil ice formation when T_o = -0.55°C are shown in Figure 7d for two temperature settings of the heated grid. Two settings for grid heating were used in order to test its effect on the rate of frazil ice formation. As is subsequently indicated in Figure 10, the heat input into the jar from the grid did not have a pronounced effect on the rate of frazil ice formation for larger temperatures of supercooling. The heat input was, however, reduced for values of T_o = -0.25°C, -0.10°C and -0.05°C, with the intention that its contribution to the heating of the jar would not dominate that of the latent heat of fusion resulting from frazil ice growth. Nevertheless, it was found (using the analytical model) that when T_o = -0.10°C and -0.05°C the heat input from the grid affected the experimental data. Because the heat input $\dot{T}$ from the grid could be accounted for in the analytical model, eq 17 through 19, the experimental data could, however, be used to both validate and calibrate the model.

From the comparison of experimental data and calculated results obtained using eq 17 through 19, and using equivalent values of $\dot{T}$, it was found that during an experiment the heat transfer coefficient α varies from an initial value of α_o to approximately one-half of its value (0.5 α_o). Correlation between experimental and analytical data led to selection of the values of the constants given in eq 19 with the following results:

$$\alpha = 0.5\,\alpha_o\,(1 + e^{-(40\,c_f)}). \qquad (28)$$

The decreasing value of the heat transfer coefficient α with time is attributable both to the increasing viscosity of the water-ice mixture as the water temperature in the turbulence jar rises and to the interference of the frazil ice particles with the heat transfer process. Frazil ice particles suspended in the fluid act to damp the turbulence eddies in the flow, thus leading to a reduction in turbulence intensity and resulting in a decline in the value of the heat transfer coefficient. Another factor contributing to the reduction in the rate of heat transfer from the frazil ice particles is that the particles agglutinate or sinter (Martin 1981) and agglomerate as flocs, thereby reducing the surface area of ice that is exposed to the water.

Predicted records of temperature rise with time are presented in Appendix C. These records were obtained from the numerical integration of eq 17 and 18 with α expressed as eq 28. In Figure C1 the same values of $\dot{T}$ were used as were used in obtaining the experimental data, but in Figure C2, $\dot{T}$ was set equal to zero. Comparison of Figures C1 and C2 for $\dot{T}$ = -0.10°C and -0.05°C shows the degree to which grid heating marked the experimental data for these values of T_o.

The frequency of grid oscillation was related to turbulence exchange coefficient ϵ in the following way. The variation with depth of the concentration of suspended fine sand particles in the turbulence jar for several frequencies of grid oscillation was plotted as is shown in Figure 8. From Figure 8, Figure 9 was plotted to obtain (in the manner

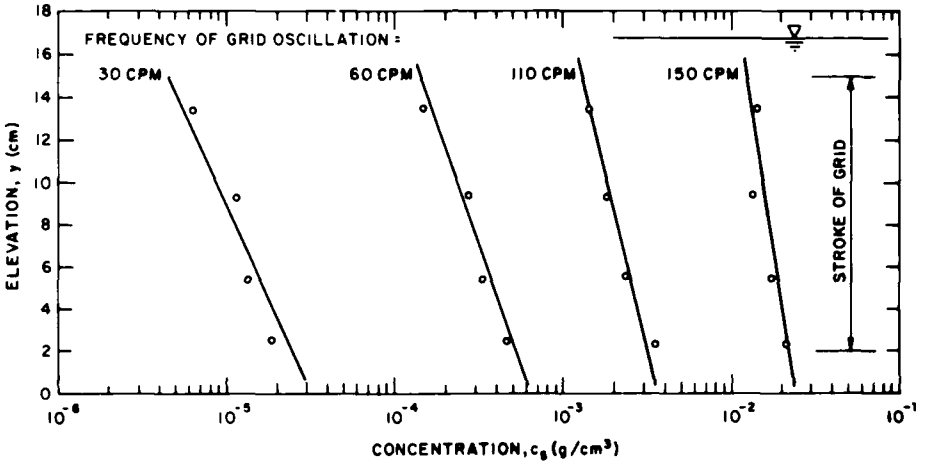

Figure 8. Distributions of suspended sediment concentration with depth in the turbulence jar versus frequency of grid oscillation F_g *(CPM–cycles per minute).*

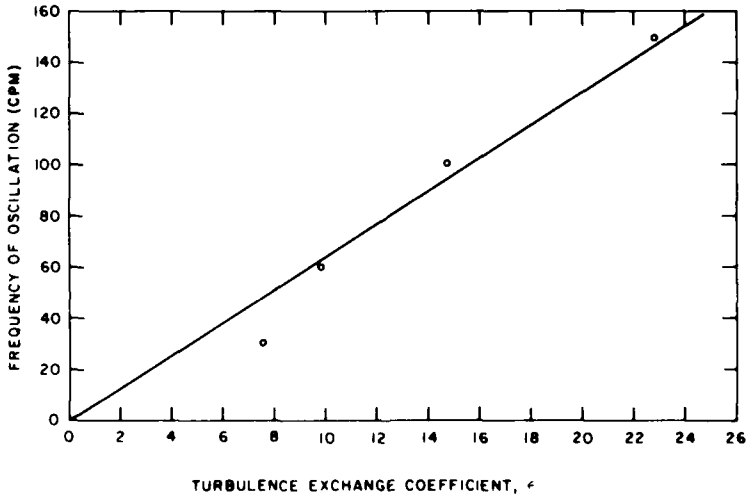

Figure 9. Relationship between frequency of grid oscillation F_g *and turbulence exchange coefficient* ϵ *(CPM - cycles per minute).*

described in the *Elements of Turbulence* section) the relationship between frequency of grid oscillation F_g and the corresponding value of turbulence exchange coefficient ϵ. It should be noted that the values of ϵ obtained for the jar are gross values. Because of the prismatic form of the turbulence jar and the shape of the oscillating grid, values of ϵ would vary somewhat from location to location within the jar.

The average temporal rate of temperature rise because of frazil ice formation in the turbulence jar T_{Frazil}, multiplied by the specific heat (or heat capacity) of water at 0°C, S_H = 4.218 kJ/kg°C, is plotted in Figure 10 against the grid oscillation F_g. The ordinate in Figure 10 is equivalent to the rate of heat release per unit weight of water because of frazil ice formation, that is

$$Q_W \simeq \rho V S_H \dot{T}_{\text{Frazil}}$$

or

$$\frac{Q_W}{\rho V} \simeq S_H \dot{T}_{\text{Frazil}} \tag{29}$$

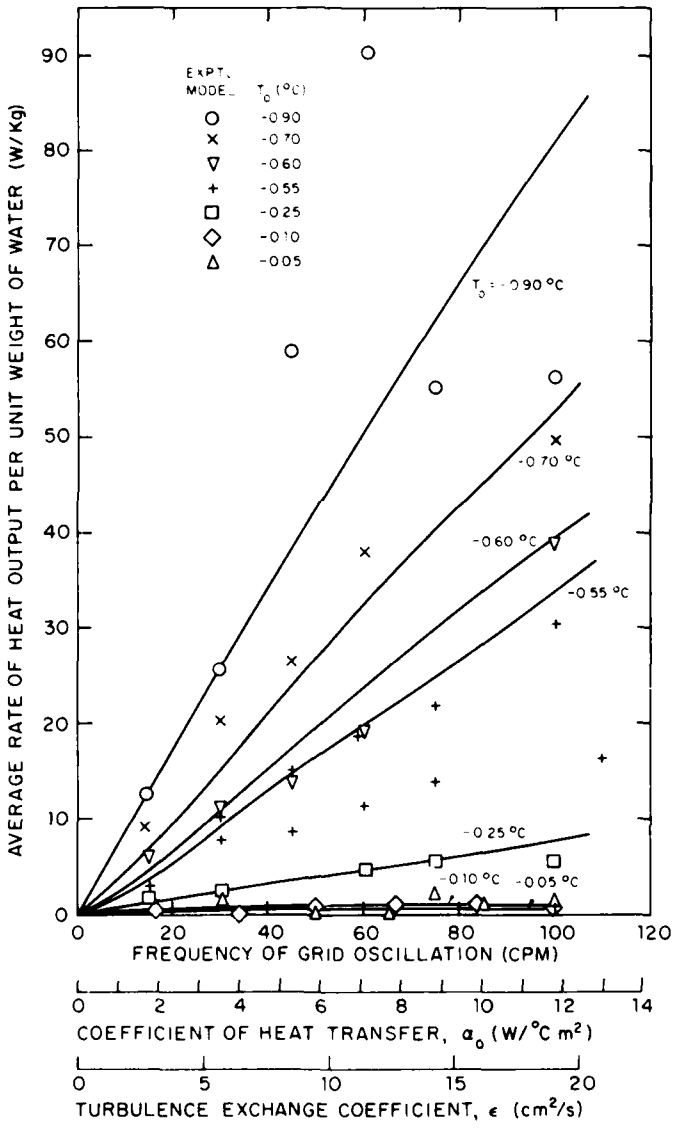

Figure 10. Average temporal rates of frazil ice formation versus frequency of grid oscillation F_g, *initial heat transfer coefficient* α_o, *and turbulence exchange coefficient* ϵ. *The curves are plotted through the analytically determined data (CPM - cycles per minute).*

where $\dot{T}_{Frazil}$ = average temporal rate of temperature rise because of frazil ice formation. The reader should bear in mind that the effect of the temperature rise from the heated grid has been removed from Figure 10. Plotted as an alternate abscissa in Figure 10 are values of the turbulence exchange coefficient ϵ determined for the frequencies of grid oscillation F_g. Also plotted in Figure 10 are the values of $S_H \dot{T}_{Frazil}$ as predicted using the analytical model of the frazil ice formation. The predicted values of $S_H \dot{T}_{Frazil}$ are plotted against the initial value of the heat transfer coefficient α_o. The abscissa of Figure 10 is composed of three scales, F_g, ϵ and α_o. The α_o scale was set so that the experimental and the analytical data coincided and the analytical model was thereby calibrated. The curves shown in Figure 10 are drawn through the values of $S_H \dot{T}_{Frazil}$ as determined using eq 17, 18 and 28. For the same values of F_g, or equivalent α_o, both the analytically predicted and the experimentally determined values of $S_H \dot{T}_{Frazil}$ are given. Although the experimental data exhibit some scatter, the analytically predicted data overlay the experimental data fairly well. Both the experimental and the calculated data are associated with equivalent values of grid heating $\dot{T}$.

It is apparent from Figure 10 that values of turbulence exchange coefficient ϵ ranging from 0 to about 20 cm^2/s correspond to initial values of heat exchange coefficient α_o ranging from 1 to 14 $W/°C\ m^2$. Figure 10 indicates that the analytical model adequately embodies the physics of frazil ice formation; the experimental and analytical data coincide quite well.

On the basis of the results given in Figure 10, it can be concluded that the average rate of frazil ice formation increases for higher levels of turbulence in a flow. However, the influence of turbulence decreases with increasing values of initial temperature of supercooled water; for values of T_o less than about 0.10°C, the level of turbulence does not appear to have a major effect on the rate of ice formation in a parcel of supercooled water that is not bounded by a free surface.

Water temperature

It is evident from both the experimental and analytical results that frazil ice forms more rapidly, and in greater amounts, in colder supercooled water. These results are graphically illustrated in Figure 11, in which the increase in water temperature attributable to the formation of frazil ice is compared for two initial temperatures of supercooling, T_o = -0.55°C and -0.90°C. For the same frequency of grid oscillation, or level of turbulence, the initially colder water is warmed at a greater rate by the greater amount of frazil ice that forms. The aforementioned variation of the amount of frazil ice formation is also depicted in Figure 12, in which the amount of frazil ice formed as estimated using the analytical model—that is using eq 17, 18 and 28—is plotted against time for parcels of water with the same value of turbulence exchange coefficient ϵ.

An inspection of eq 17 reveals that the rate of temperature rise (i.e. the rate of frazil ice formation) is a quadratic in T. Consequently, the lower the temperature of supercooling T_o, and hence the initial values of T, the greater the rate of frazil ice formation.

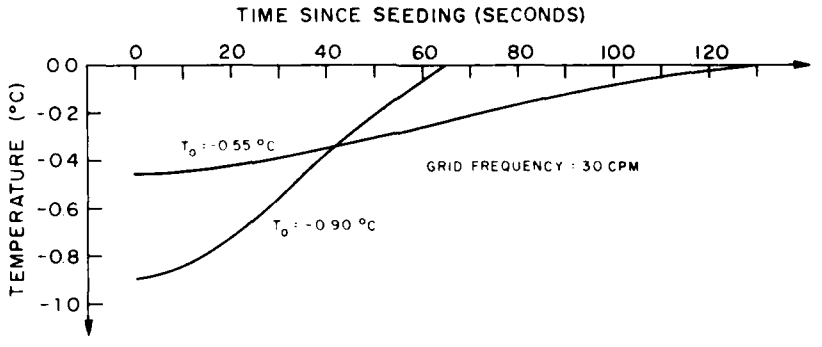

Figure 11. Comparison of rates of temperature rise attributable to frazil ice formation for two initial temperatures of supercooled water and similar levels of turbulence (CPM–cycles per minute).

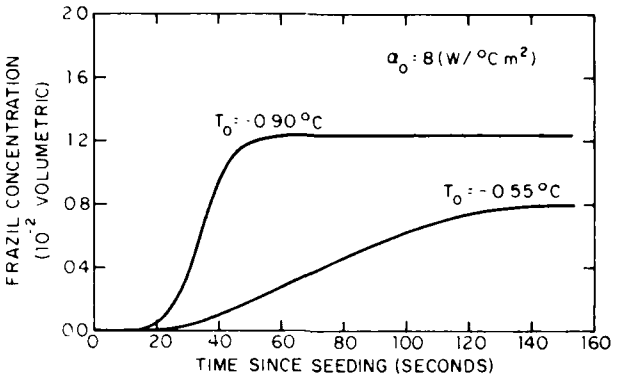

Figure 12. Comparison of rates of frazil ice formation for two initial temperatures of supercooled water and similar levels of turbulence.

Influences of water temperature and turbulence on the concentration of frazil ice

The concentration of frazil ice as a function of time for several temperatures of supercooling and initial values of the heat transfer coefficient are given in Figure 13. The curves in Figure 13 were determined using the analytical model, that is, eq 17 with $\dot{T}$ set as zero and eq 18 and 28 calibrated to the experimental results (Fig. 10). The average temporal rates of frazil ice formation, calculated as the final volume of frazil ice divided by the time for the water temperature to reach 0°C, are plotted with α_o and ϵ and are presented in Figure 14.

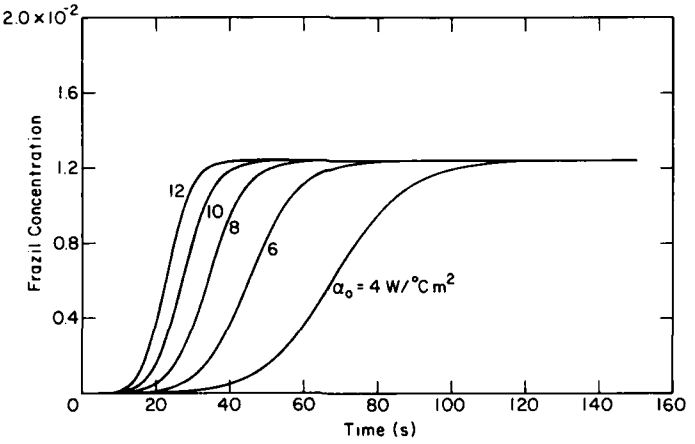

a. $T_o = -0.90°C$.

Figure 13. Temporal variation in frazil ice concentration for different values of initial heat transfer coefficient, α_o ($\dot{T} = 0$).

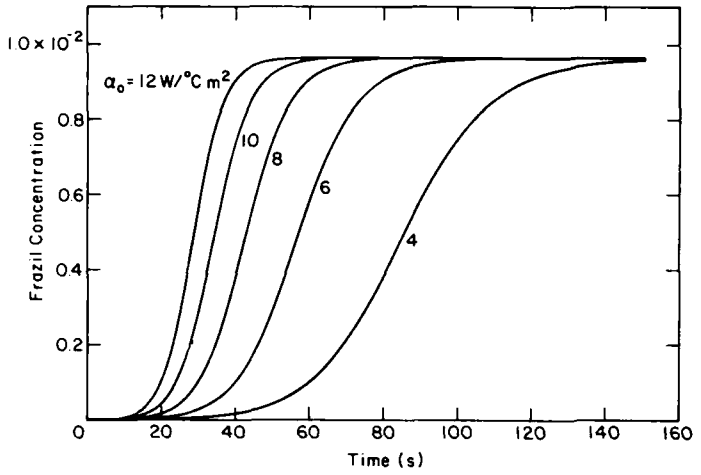

b. $T_o = -0.70°C$.

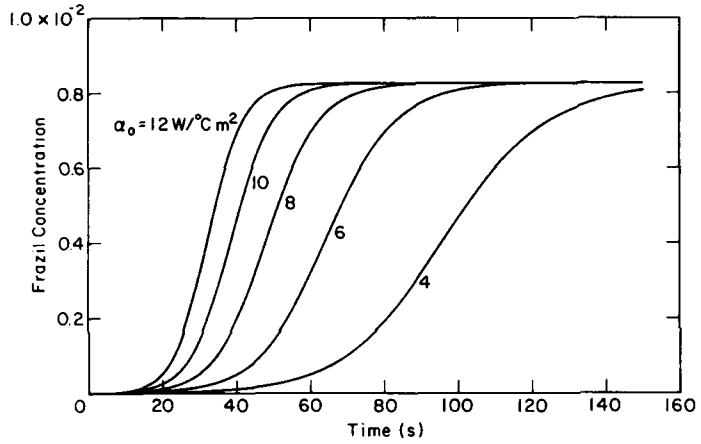

c. $T_o = -0.60°C$.

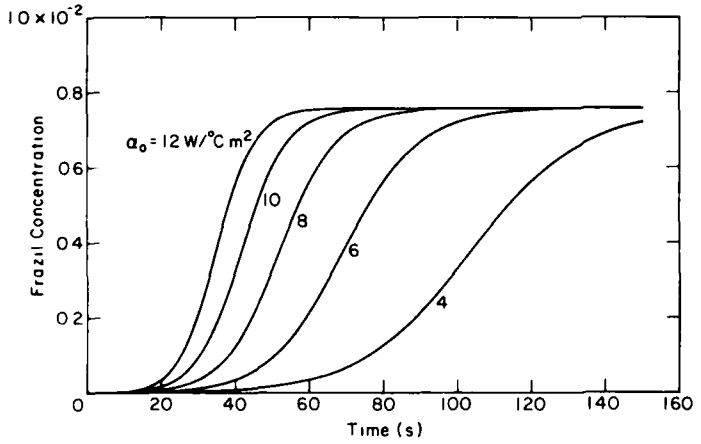

d. $T_o = -0.55°C$.

Figure 13 (cont'd). Temporal variation in frazil ice concentration for different values of initial heat transfer coefficient, α_o ($\dot{T} = 0$).

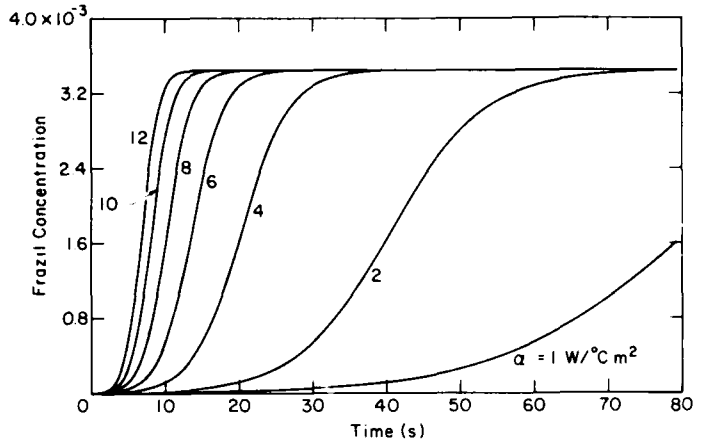

e. $T_o = -0.25°C$.

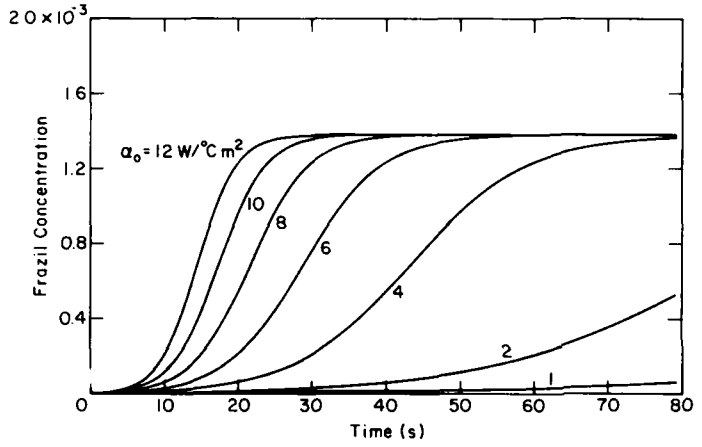

f. $T_o = -0.10°C$.

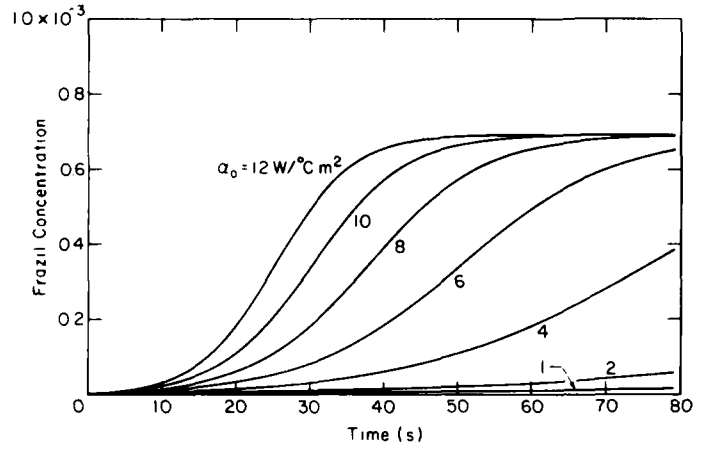

g. $T_o = -0.05°C$.

Figure 13 (cont'd).

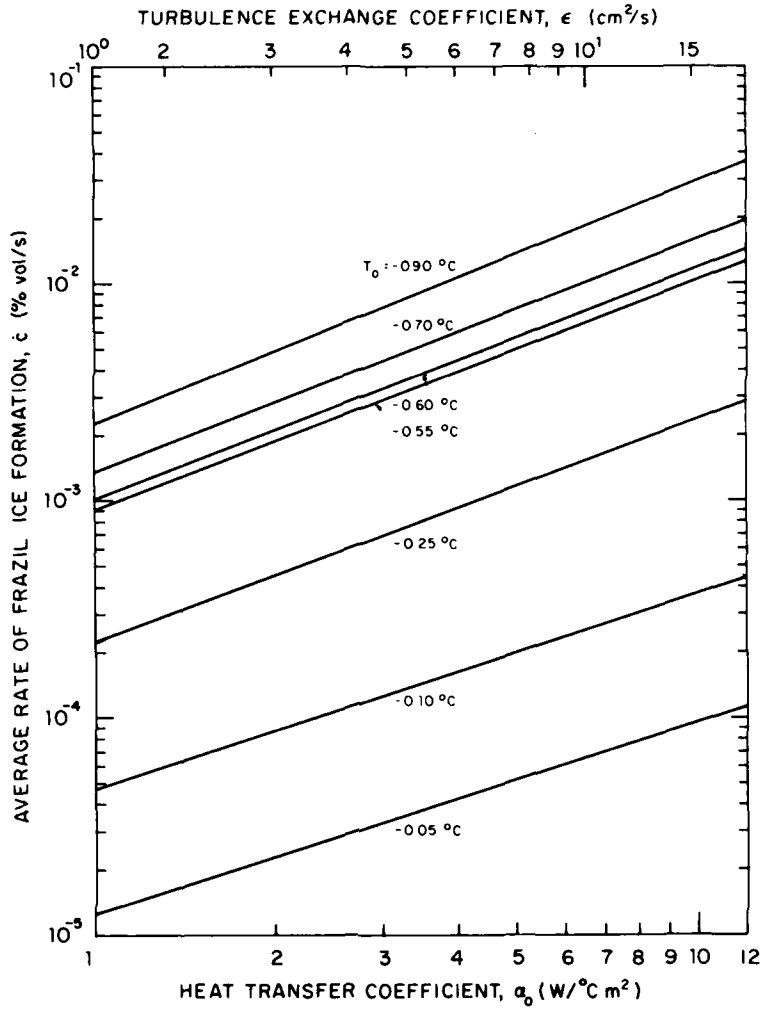

Figure 14. Variation of the average rate of frazil ice formation with temperature of supercooling T_o, initial value of heat transfer coefficient α_o and turbulence exchange coefficient ϵ.

With larger initial temperatures of supercooling T_o, both the rate of frazil ice formation and the final concentration of frazil ice increase. The temporal rate of frazil ice formation (measured as volumetric concentration) also increases with increasing values of turbulence exchange coefficient, that is, with increasing turbulence intensity. It is evident from Figure 14 that the following relationship exists between $\dot{c}$, ϵ and T_o:

$$\dot{c} = \epsilon^n f(T_o) \qquad (30)$$

where $n \simeq 1.0$ for all values of T_o. In other words, the average rate of frazil ice formation is directly proportional to the turbulence intensity of the fluid in which it forms. The average rate of frazil ice formation is strongly related to the initial temperature of supercooling T_o.

No measurements were made of the actual concentration of frazil ice that formed in the turbulence jar. A review of the present techniques for measuring frazil ice concentration (for example, that proposed by Tsang 1977) showed that these techniques require further development before they can be used. The concentration of frazil ice, for this study, was determined analytically by way of the heat produced and the attendent water temperature rise accompanying frazil ice formation. The analytical model indicates that the final concentration of frazil ice for a given temperature of supercooling T_o is independent of the turbulence regime of the flow. Turbulence affects the rate of frazil ice formation but not its final concentration. Turbulence may indirectly

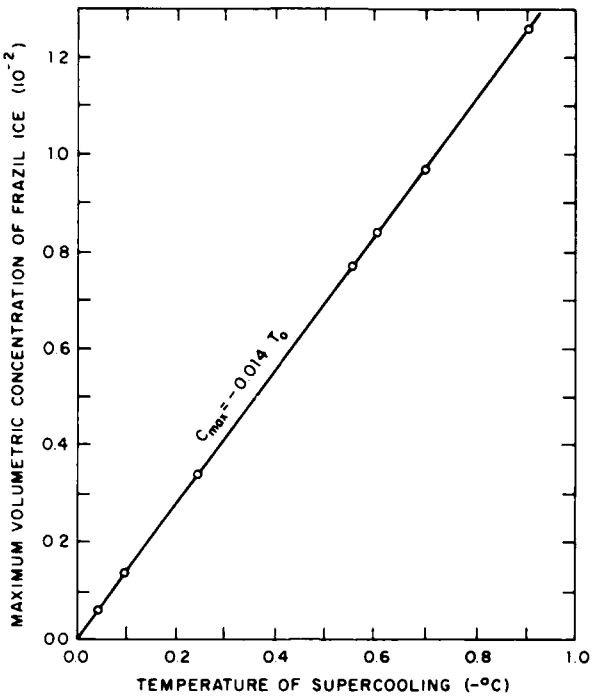

Figure 15. Variation of the final concentration of frazil ice with temperature of supercooling T_o.

influence the amount of frazil ice formed by enabling a body of water to become supercooled to a lower temperature *prior* to nucleation. The final values of frazil ice concentration c_{max} are plotted in Figure 15 against T_o. In keeping with the formulation of the analytical model, the values of c_{max} are directly proportional to T_o. On the basis of the analytical model, calibrated with the experimental data, the following relationship can be proposed for c_{max}

$$c_{max} = -0.014\ T_o \qquad (31)$$

where c_{max} = maximum volumetric concentration of frazil ice produced in supercooled water and T_o = minimum temperature below freezing (°C) of the supercooled water. Equation 31 is essentially the theoretical limit for the concentration of ice formed in a parcel of supercooled water. This limit can be estimated by equating the quantity of ice that is required to raise the water temperature to 0°C by way of release of latent heat of fusion L_i. That is,

$$c_{max} = -\frac{\rho S_H T_o}{\rho_i L_i} = -0.014\ T_o \qquad (32)$$

where ρ and ρ_i = the densities of liquid water and ice at the temperature of supercooling T_o, S_H = specific heat of water, 4.218 kJ/kg°C and L_i = latent heat of fusion of ice, 333.6 kJ/kg. For river water supercooled to about -0.1°C, eq 31 gives a maximum volumetric concentration of frazil ice of 0.14%. This value is approximately one quarter of the value that was reported by Tsang (1982), who cites a maximum volumetric concentration of 0.55 % for rivers (from Ontario Hydro 1970). The disparity in the two values may have one of several causes. The field value, cited by Tsang, was evaluated from samples taken from the upper portion of flow in the Niagara River. Observed concentrations of frazil ice are likely to be higher in the upper portion of a flow because of the influence of buoyancy that causes frazil ice particles to rise toward the surface. An additional possible cause is that the river may continuously lose heat to frigid air, thereby enabling frazil ice formation to continue. Larger concentrations of frazil ice may occur when the particles agglutinate and locally agglomerate into slush ice; slush ice, however, forms as a consequence of the transport and mechanical concentration of frazil ice by the flow and is only indirectly dependent on the formation of frazil ice from a supercooled parcel of water.

Frazil ice particle shape and size

Measurements of the particle size of frazil ice showed that maximum particle size, both in terms of the length of the longest axis and the surface area,

increases with decreasing initial water temperature T_0 and decreases with increased turbulence intensity.

Frazil ice particles as single crystals and as agglutinated or sintered laminations of crystals were observed and measured. Size distributions of frazil ice particles were not determined. Larger frazil ice particles can form in initially colder water because of the more rapid rate of frazil ice formation and longer period for growth. At the higher turbulence intensities, a limiting size of frazil ice particles is reached because the turbulence eddies act to buffet, flex and break those particles that get large. Measured values of maximum particle length or diameter (as defined in the sketches in Fig. 16) of observed frazil ice

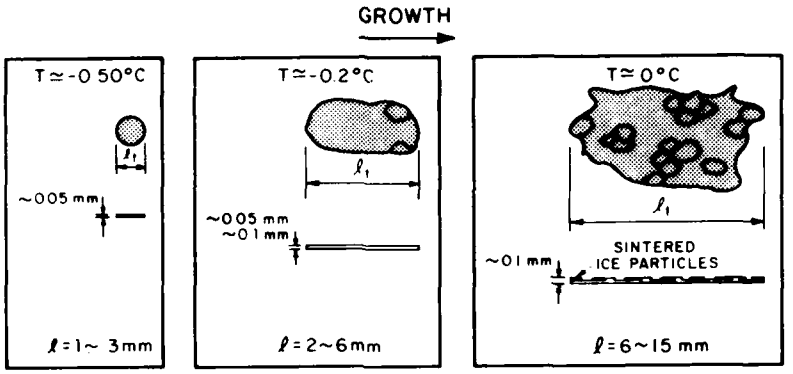

Figure 16. Summary of sizes and shapes of frazil ice particles observed when temperature of supercooling was -0.55°C.

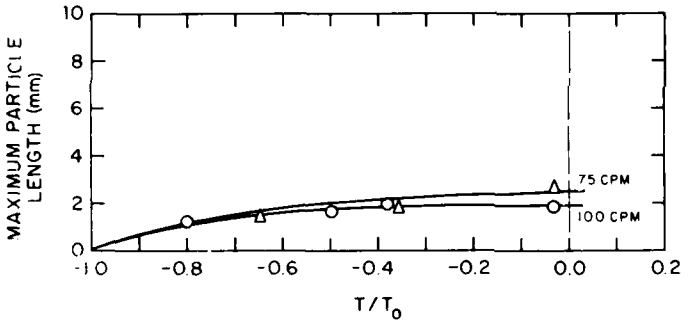

a. $T_o = -0.05°C.$

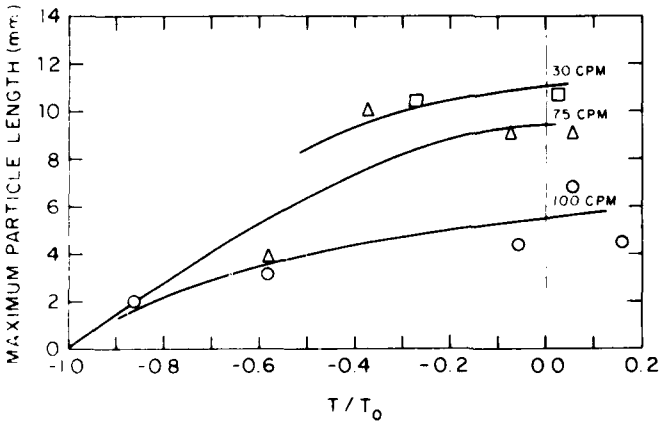

b. $T_o = -0.25°C.$

Figure 17. Measured values of maximum diameter of frazil ice particles versus water temperature normalized by temperature of supercooling T_o (CPM–cycles per minute).

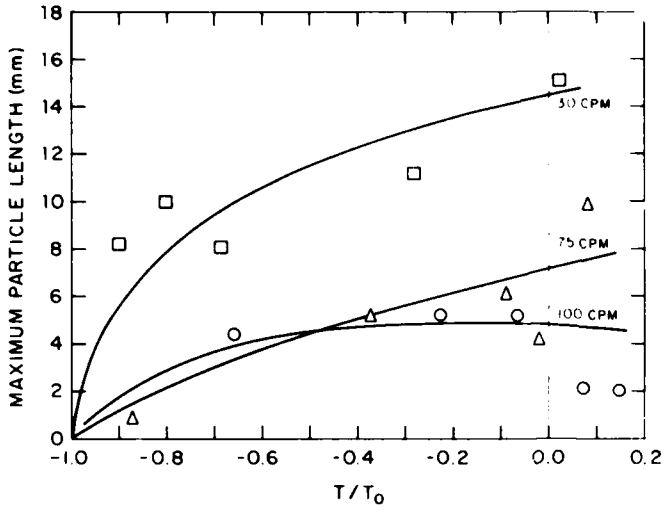

c. $T_o = -0.55°C$.

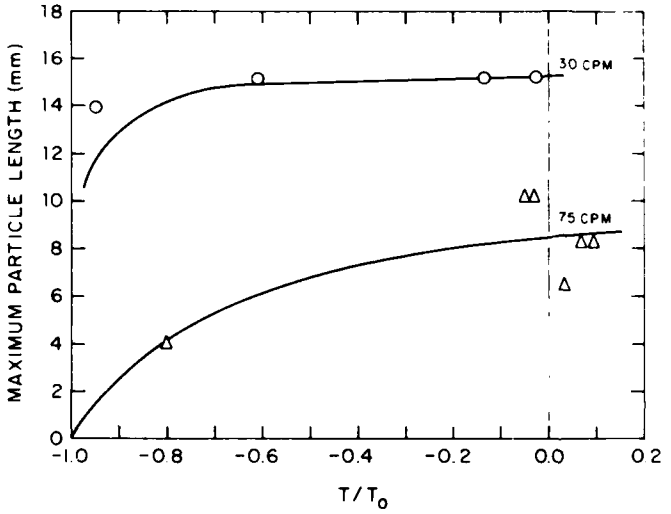

d. $T_o = -0.70°C$.

Figure 17 (cont'd).

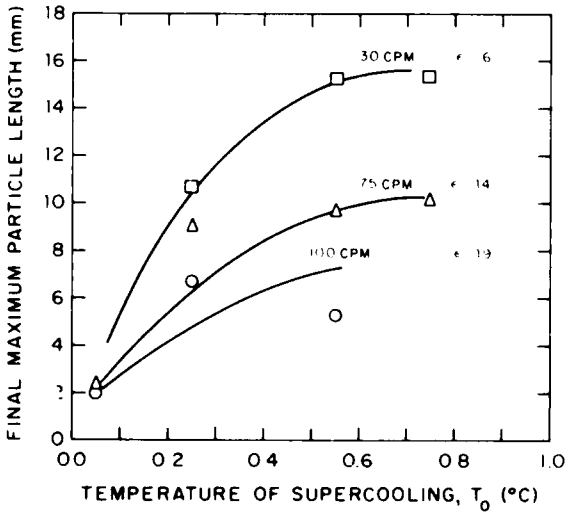

Figure 18. Final maximum length, or diameter, of frazil ice particles versus temperature of supercooling T_o *(CPM–cycles per minute).*

particles are plotted in Figure 17 against water temperature that is normalized by initial temperature of supercooling T/T_o. The final maximum lengths of frazil ice particles are plotted in Figure 18 against temperature of supercooling, with turbulence exchange coefficient ϵ as a third parameter. The trend of increasing frazil ice particle size with decreasing level of turbulence is evident in Figure 18.

When the temperature of supercooling was less than about -0.10°C, the frazil ice particles had the form of disks with maximum diameter of approximately 2 to 3 mm and thickness of about 0.05 mm. For water supercooled to initially lower temperatures, the frazil ice particles had sufficient time to grow to a larger size and to become more irregular in shape (see Fig. 16). Occasionally, the larger frazil ice particles would have smaller particles (single crystals) about 1 mm in diameter fused or sintered to their surfaces.

CONCLUSIONS

A study involving experimentation coupled with an analytical model of frazil ice formation in a supercooled parcel of water was conducted in order to investigate the influences of turbulence and water temperature on frazil ice formation. The following conclusions were drawn from the study.

Ice fragments or crystals are required to seed water that has been supercooled to temperatures as low as -0.9°C. Chilled, nonaqueous particles placed in supercooled water do not cause frazil ice to develop.

The most important determinant of frazil ice formation is the initial temperature of supercooling. Both the formation rate and the concentration of frazil ice increase with lower temperatures of supercooling. A simple relationship exists between the temperature of supercooling and the maximum concentration of frazil ice that can be formed in a volume of supercooled water.

The rate of frazil ice formation is directly proportional to intensity of turbulence of the fluid in which it is forming. The turbulence characteristics of a flow affect the rate of frazil ice formation by governing the temperature to which the flow can be initially supercooled, by influencing the processes of heat transfer from the crystals to the surrounding water, and by promoting collision nucleation and floc rupture and thereby increasing the number of nucleation sites.

Results from the analytical model suggest that the final concentration of frazil ice, for a given temperature of supercooling, is independent of the turbulence intensity of flow.

Larger frazil ice particles (crystals and platelets of fused crystals) form in water supercooled to lower temperatures, but particle size decreases with increasing turbulence intensity. Large frazil ice particles, having a major platelet diameter of about 10 mm and a thickness of about 0.1 mm or less, tend to be broken when jostled by flow eddies.

For temperatures of supercooling of -0.10°C and less, as are typically recorded for supercooled water in rivers and streams, the maximum length of the frazil ice disks was found to be about 2 mm.

LITERATURE CITED

Altberg, W.J. (1936) Twenty years of work in the domain of underwater ice formation. *International Association of Scientific Hydrology*, Bulletin No. 23, pp. 373-407.

Andres, D.D. (1982) Nucleation and frazil ice production during the supercooling period. In *Proceedings of the Workshop on Hydraulics of Ice-Covered Rivers, June, Edmonton, Alberta*, pp. 168-175.

Arakawa, K. (1954) Studies on the freezing of water. *International Association of Scientific Hydrology*, Publication No. 39, pp. 474-477.

Arden, R.S. and T.E. Wigle (1972) Dynamics of ice formation in the Upper Niagara River. In *International Symposium on the Role of Snow and Ice in Hydrology, Banff, Alberta.* UNESCO-WHO-IAHS, vol. 2, pp. 1296-1312.

Barnes, H.T. (1928) *Ice Engineering.* Montreal, Canada: Renouff Publishing Company.

Carstens, T. (1966) Experiments with supercooling and ice formation in flowing water. *Geofysiske Publikasjoner*, **26**(9): 1-18.

Carstens, T. (1970) Modelling of ice transport. In *Proceedings of IAHR Symposium on Ice and Its Action on Hydraulic Structures, September, Reykjavik*, paper no. 4.15.

Devik, O. (1931) Thermische und Dynamische Bedingungen der Eisbildung im Wasserlaufen. *Geofysiske Publikasjoner*, **9**(1).

Dorsey, N.E. (1948) The freezing of supercooled water. *Transactions of the American Philosophical Society*, **38**(3): 245-328.

Garabedian, H. and R.F. Strickland-Constable (1974) Collision breeding of ice crystals. *Journal of Crystal Growth*, **22**: 188-192.

Granbois, K.J. (1953) Combatting frazil ice in hydroelectric stations. *Power Apparatus and Systems*, **5**: 111-116.

Hanley, T.O'D. and B. Michel (1977) Laboratory formation of border ice and frazil shush. *Canadian Journal of Civil Engineering*, **4**: 153-160.

Hobbs, P.V. (1974) *Ice Physics.* London: Oxford University Press.

Kumai, M. and K. Itagaki (1954) Cinematographic study of ice crystal formation in water. *International Association of Scientific Hydrology*, Publication No. 39, pp. 463-467.

Martin, S. (1981) Frazil ice in rivers and oceans. *Annual Review of Fluid Mechanics*, **13**: 379-397.

Martin, S. and P. Krauffman (1981) A Field and laboratory study of wave damping by grease ice. *Journal of Glaciology*, 27(96): 283-314.

Matousek, V. (1981) A mathematical model of the discharge of frazil in rivers. In *IAHR International Symposium on Ice, July, Quebec, Canada*, pp. 81-99.

Michel, B. (1967) From the nucleation of ice crystals in clouds to the formation of frazil ice in rivers. In *Proceedings of International Conference on Low Temperature Science, Hokkaido University, Sapporo, Japan*, pp. 129-136.

Michel, B. (1972) Properties and processes of river and lake ice. In *International Symposium on the Role of Snow and Ice in Hydrology, September, Banff, Alberta.* UNESCO-WHO-IAHS, pp. 454–481.

Michel, B. (1978) *Ice Mechanics.* Laval, Quebec: Les Presses de L'University.

Mueller, A. (1978) Frazil-ice formation in turbulent flow. The University of Iowa, Iowa Institute of Hydraulic Research, Report No. 214.

Mueller, A. and D.J. Calkins (1978) Frazil ice formation in turbulent flow. U.S.A. Cold Regions Research and Engineering Laboratory, Miscellaneous Publication 1135.

Ontario Hydro (1969) Niagara River ice. In Study of River and Lake Ice. I.H.D. Project No. C.6.7, File Reference: R-SIG-6; Ontario-27, Progress Report No. 4, December.

Osterkamp, T.E. (1978a) Frazil ice formation: A review. *Journal of the Hydraulics Division, ASCE,* **104**(HY9): 1239-1255.

Osterkamp, T.E. (1978b) Frazil ice nucleation mechanisms. Scientific Report, Geophysical Institute of Alaska.

Osterkamp, T.E. and J.P. Gosink (1981) A photographic study of frazil ice formation in streams and rivers. *Second Workshop on Hydraulics of Rivers, June, Edmonton, Alberta,* pp. 131-147.

Rouse, H. (1937) Modern conception of the mechanics of fluid turbulence. *Transactions, ASCE,* **102**: 532-536.

Rouse, H. (1938) Experiments on the mechanics of sediment suspension. In *Proceedings of the Fifth International Congress of Applied Mechanics, Cambridge, Massachusetts,* pp. 550-554.

Schaeffer, V.J. (1950) The formation of frazil and anchor ice in cold water. *Transactions, American Geophysical Union,* **31**(6).

Tesaker, E. (1975) Accumulation of frazil ice in an intake reservoir. In *Proceedings of the IAHR International Symposium on Ice,* pp. 25-38.

Tsang, G. (1977) Development of an experimental frazil ice instrument. In *Proceedings of Third National Hydrotechnical Conference, May, Quebec.* Canadian Society of Civil Engineers, pp. 671-692.

Tsang, G. (1982) *Frazil and anchor ice: A monograph.* Ottawa: National Research Council of Canada, Associate Committee of Hydrology, Subcommittee of Hydraulics of Ice-Covered Rivers.

Wigle, T.E. (1970) Investigations into frazil, bottom ice and surface ice formation in the Niagara River. In *Proceedings of IAHR International Symposium on Ice and Its Action on Hydraulic Structures, September, Reykjavik,* paper no. 2.8.

Williams, G.P. (1959) Frazil ice: A review of its properties with a selected bibliography. *Engineering Journal,* **42**(11): 55-60.

APPENDIX A: PRELIMINARY FRAZIL ICE EXPERIMENTS

Flume experiments

A series of experiments was conducted using the Iowa Institute of Hydraulic Research (IIHR) 40-ft-long (12 m) refrigerated flume that used several means of ice crystal seeding to start nucleation. The object was to obtain major growth of frazil ice during the passage of the flow through the labyrinth channel formed by placing two partitions in the 2-ft-wide (0.6 m) flume to form a 120-ft-long (37 m), 8-in.-wide (0.2 m) channel.

In the earlier experiments with seeding near the upstream end of the channel, it was repeatedly observed that little frazil was formed along the 120-ft-long (37 m) channel, but frazil ice was formed and the supercooling exhausted after the flow then passed through the pump and the return pipe. Thereafter, various attempts were made to nucleate the supercooled flow near the downstream end of the channel. After the passage of the seed ice through the pump and the return pipe, a large amount of frazil ice appeared at the upstream end of the flume. Apparently, the agitation of passage through the pump and return pipe led to formation of sufficient frazil to exhaust the supercooling before the flow entered the open-channel portion of the flow circuit.

In an attempt to obtain a more rapid formation of frazil ice, experiments were made in which the supercooled flow was seeded with a "slug" of frazil ice, with the objective of providing more nucleation centers. This was done by supercooling water in the turbulence jar (described in the *Analytical Model* section), nucleating it with ice and injecting a portion of the resultant frazil-water mixture into the flow at the upstream end of the channel. During repeated runs there was, as frazil passed a temperature probe, a temporary rise in local temperature in the downstream direction along the channel. After careful evaluation of this seemingly encouraging result, it was suspected that much of the temperature rise resulted from diffusion of the 0°C liquid water introduced with the frazil ice near the upstream end of the flume. Fortunately (or unfortunately) this suspicion was confirmed when only frazil ice particles from the turbulence jar, instead of the frazil-liquid water mixture, was used for nucleation. In these experiments there was no appreciable amount of frazil ice formation or temperature rise along the channel. The first sizable quantity of frazil that appeared was observed at the upstream end of the channel, after passage of the seeded flow through the pump and the return pipe.

So, the partitions were removed from the flume and experiments were made in a high velocity, shallow supercritical flow in an effort to enhance the rates of floc formation and loss of supercooling. However, any increase in these effects was more than offset by the reduced residence time of the nucleated water in the working section of the flume.

In summary, the IIHR flume proved to be unsuitable for conducting experiments to accomplish the goals of the study.

Couette-flow

In the quest for an apparatus that would give an endless turbulent shear-layer flow, which is virtually free of the end effects that plagued the refrigerated flume, a series of experiments was conducted using a couette-flow annulus. The annulus was made from 0.5-in.-diameter (1.3 cm) tubing and had a major diameter of about 8 in. (20 cm). It was equipped with two short radial nipples through which the annulus could be filled with water and nucleated. The annulus was attached to a horizontal axle through its principal center of curvature and the axle, in turn, was attached to a variable-speed motor. The lower one-third of the annulus was immersed in a temperature-controlled salt water ice bath. The annulus was filled to mid-depth with supercooled water, then nucleated with ice crystals through one of the nipples.

The frazil ice that formed subsequently was found to adhere tenaciously to the walls of the annulus and was then swept through the sheared flow in the lower part of the annulus as it rotated. After a few experiments it was concluded that this "forced advection" of the frazil ice through the liquid was having the same effect on frazil formation as the transport of the frazil through liquid water in the early turbulence jar experiments with an unheated grid, and was therefore completely dominating the normal particle diffusion and floc growth process. The couette-flow annulus experiments were abandoned.

APPENDIX B: LISTING OF COMPUTER PROGRAM FOR CALCULATION OF FRAZIL ICE FORMATION

```
// EXEC FORTHCLG,REGION=200K
//FORT.SYSIN DD *
C      ALPH=HEAT TRANSFER COEFFICIENT
C      RO=DENSITY OF WATER
C      ROI=DENSITY OF ICE
C      AI=LATENT HEAT OF FUSION OF ICE
C      BI=CHAR.LENGTH OF ICE PARTICLE(THICKNESS)
C      SH=SPECIFIC HEAT OF ICE
C      TR=RATE OF HEATING BY GRID
C      TO=INITIAL TEMPERATURE OF  SUPERCOOLED WATER
C      TM=EQUILIBRIUM TEMPERATURE OF ICE AND WATER
C      TEMP=WATER TEMPERATURE AT ANY TIME
C      T=TIME,IN SECONDS
C      V=VOLUME OF TURBULENCE JAR
C      J IS A COUNTER
       DIMENSION ALPH(260),CO(260),AB(260),TC(260),B(260),T1(260)
       DIMENSION C1(260),T(260),X(260),TEMP(260),A(260),A1(220),A2(220)
       DOUBLE PRECISION T,F,X,TEMP,A,E,Q,AB,B,ALPH,TC,CO
       COMMON ROI,RO,AI,BI,TR,TO,SH,V,D,TM
C
C      N1=NO. OF ALPHA'S
C      N2=NO. OF TO'S
       READ(5,3) N1,N2
       READ(5,4) (A1(K1),K1=1,N1)
       READ(5,4) (A2(K2),K2=1,N2)
3      FORMAT(4I5)
4      FORMAT(6F10.2)
       DO 2000 IJ=1,2
       DO 1000 I1=1,N2
       DO 500 II=1,N1
C      INITIALISE T,TEMP,X,A,N
       N=1
       J=1
       M=0
       TO=A2(I1)
       TM=0.00
       H=2.0
       IF(II.GT.5) H=8.0
C
       T(J)=0.000
       TEMP(J)=TO
       X(J)=TEMP(J)-TM
       A(J)=0.0002
       V=0.004128
       CO(J)=0.00
C
C      COMPUTE STEP CONSTANTS B, C, D,
       ALPH(J)=A1(II)
       IF(IJ.EQ.1) WRITE(6,5) TO,ALPH(1)
       RO=999.0
       ROI=917.00
       AI=333.60
       SH=4.2177
       BI=0.0001
       TR=0.00020
       IF(I1.EQ.1) TR=.00042
       IF(I1.EQ.2) TR=.00085
```

```
      IF(I1 EQ 3) TR= 00071
      IF(I1 EQ 4) TR= 000625
      IF(I1 EQ 5) TR=.000552
      IF(I1.EQ.6) TR= 000522
      IF(I1 EQ 7) TR= 000459
      B(J)=ALPH(J)*TR/(RO1*A1*B1)
      TC(J)=S(J)/TR
      D=TR
      AB(J)=(ALPH(J)/(RO*CH*V))*(A(J)+RO*CH*V*(TM-TO)/(RO1*A1*B1))
      F=D-X(J)*X(J)*TC(J)-AB(J)*X(J)
C     WRITE(6,100) B(J),TC(J),AB(J),ALPH(J)
100   FORMAT(/,5X,E12.5,4X,E12.5,4X,E12.5,4X,E12.5,4X,E12.5)
C
C     CALL ON THE RUNGE KUTTA SOLUTION METHOD TO
C     SOLVE THE GOVERNING EQUATION
C     WRITE (6,101) X(1)
101   FORMAT(F12.5)
      IF(X(J) LQ. 70. ) GO TO 20
13    CALL RUNGE (N,T,F,X,H,M,K,J,A,TEMP,AB,B,ALPH,TC,CO)
      N=1
      GO TO (14,20),K
C     GOVERNING EQUATION
14    F=((B(J)*T(J))-AB(J))*X(J)-TC(J)*X(J)*X(J)+D
      GO TO 13
C
C     WRITE OUT THE RESULTANT TIME
C     WRITE (6,200)J,X(J),T(J),A(J),F
20    CONTINUE
200   FORMAT (/,5X,I3,4X,F12.5,4X,F12.5,4X,E12.5,4X,F12.5)
C
      IF(X(J).GT.0.00000) GO TO 21
C     MOVE TO NEXT TEMPERATURE STEP
      J=J+1
C     IF(J.GT.100) GO TO 21
      A(J)=A(J-1)
      X(J)=X(J-1)
      T(J)=T(J-1)
      TC(J)=TC(J-1)
      B(J)=B(J-1)
      AB(J)=AB(J-1)
      ALPH(J)=ALPH(J-1)
      GO TO 13
C
C     END OF MARCHING PROCESS
21    CONTINUE
C
C     IPLOT=1 FOR PLOTTING TEMP. VS. TIME GRAPH
C     IPLOT=2 FOR PLOTTING CONCN. VS. TIME GRAPH
      IF(IJ.EQ.1) IPLOT=1
      IF(IJ.EQ.2) IPLOT=2
C     WRITE(6,5) TO,ALPH(1)
5     FORMAT(//,10X,40('*'),//,15X,'TO=',F7.3,4X,'ALPHA=',F6.1,//,
     * 10X,40('*'),//)
      IF(IJ.EQ.1) WRITE(6,1)
      IF(IJ.EQ.1) WRITE(6,2) (T(L),CO(L),X(L),L=1,J)
      J=J-1
      DO 60 L=1,J
      T1(L)=T(L)
      IF(IPLOT.EQ.1) C1(L)=X(L)
      IF(IPLOT.EQ.2) C1(L)=CO(L)

60    CONTINUE
1     FORMAT(//,13X,'TIME(SECONDS)',7X,'CONCN.(CO)',10X,'TEMPERATURE',//)
2     FORMAT(14X,F7.2,10X,E12.5,10X,E12.5)
      IF(IPLOT.EQ.1.AND.IJ.EQ.1) CALL GRAPH(J,T1,C1,11,21,0.0,5.5,
     @ 0.0,0.0,0.0,0.0,'TIME IN SECONDS',',TEMPERATURE(CENT.)',',
     @ 'TEMP. VS. TIME GRAPH',',',' )
```

```
      IF(IPLOT.EQ.2.AND.II.EQ.1) CALL GRAPH(J,T1,C1,11,21,0.0,5.5,
     1 0.0,0.0,0.0,0.0,
     * 'TIME IN SECONDS,','BRAZIL CONCN.,',
     * 'CONCN.VS.TIME GRAPH,',',',')
      IF(II.GT.1) CALL GRAPHS(J,T1,C1,11,21,';')
500   CONTINUE
1000  CONTINUE
2000  CONTINUE
      STOP
      END
C ------------------------------------------------------------------------
      SUBROUTINE RUNGE (N,T,F,X,H,M,K,J,A,TEMP,AB,B,ALPH,TC,CO)
C     THIS ROUTINE PERFORMS A RUNGE-KUTTA CALCULATION
C     BY GILLS METHOD
      DIMENSION       ALPH(260),AB(260),B(260),CO(260),TC(260)
      DIMENSION T(260),X(260),A(260),TEMP(260)
      DOUBLE PRECISION T,F,X,TEMP,A,E,Q,AB,B,ALPH,TC,CO
      COMMON ROI,RO,AI,BI,TR,TO,SH,V,D,TM
      N=1
      M=M+1
      GO TO (1,4,5,3,7 ),M
1     Q=0.00000
      E=0.5
      GO TO 9
3     E=1.00+1.00/SQRT(2.0)
4     T(J)=T(J)+0.5*H
5     X(J)=X(J)+E*(F*H-Q)
      Q=2*E*H*F+(1.0-3.0*E)*Q
      E=1.00-1.00/SQRT(2.0)
      GO TO 9
7     X(J)=X(J)+H*F/6-Q/3
      TEMP(J)=X(J)+TM
C ------------------------------------------------------------------------
      A(J)=A(1)+RO*SH*V*(TEMP(J)-TO-(TR*T(J)))/(ROI*AI*BI/2.0)
      C2=RO*SH*(TEMP(J)-TO-(TR*T(J)))/(ROI*SH)
C     A(J)=A(1)/(1.0-C2)
      CO(J)=A(J)*BI/V/2
C     WRITE(6,11) CO(J),A(J),TEMP(J),H,F,Q
11    FORMAT(/,5X,'****** CO=',F12.4,2X,'A=',F12.4,2X,'TEMP=',F10.4,
     * 2X,'H=',F10.4,/,5X,'F=',F10.4,2X,'Q=',F10.4,/)
      ALPH(J)=ALPH(1)*0.5*(1.000000+1.000000/DEXP(40.*CO(J)))
C     WRITE (6,102) ALPH(J)
102   FORMAT(F12.5)
      B(J)=ALPH(J)*TR/(ROI*AI*BI)
      TC(J)=B(J)/D
      AB(J)=(ALPH(J)/(RO*SH*V))*(A(1)+RO*SH*V*(TM-TO)/(ROI*AI*BI))
      M=0
      K=2
      GO TO 10
9     K=1
10    RETURN
      END
//GO.FT14F001 DD UNIT=SYSSQ,
// DISP=(,PASS),DSN=&&SM,SPACE=(800,(450,50)),
// DCB=(RECFM=VBS,BLKSIZE=800,LRECL=796)

//GO.SYSIN DD *
    7    7
 12.      10.        8.         6.         4.          2.
  1.
 0.90      0.70      0.60      -0.55      -0.25      -0.10
 0.05
/*
//PLOT EXEC SIMPLOT
//SYSIN DD *
BRAZIL ICC STUDY
/*
//
```

APPENDIX C: WATER TEMPERATURE RISE ATTRIBUTABLE TO FRAZIL ICE FORMATION AS COMPUTED USING THE ANALYTICAL MODEL.

Figure C1 shows experiments with grid heating; Figure C2 shows experiments without grid heating.

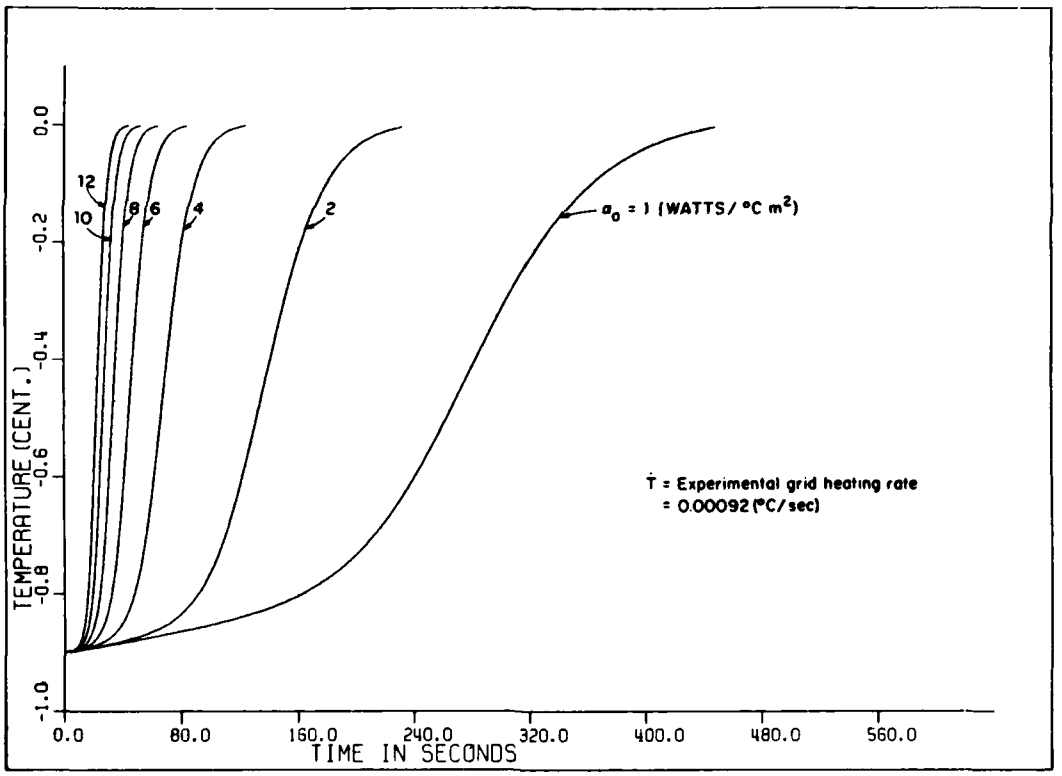

a. $T_o = -0.90°C$.

Figure C1. Variation of temperature rise attributable to frazil ice formation with initial value of heat transfer coefficient, α_o. *Initial temperature of supercooling is* T_o.

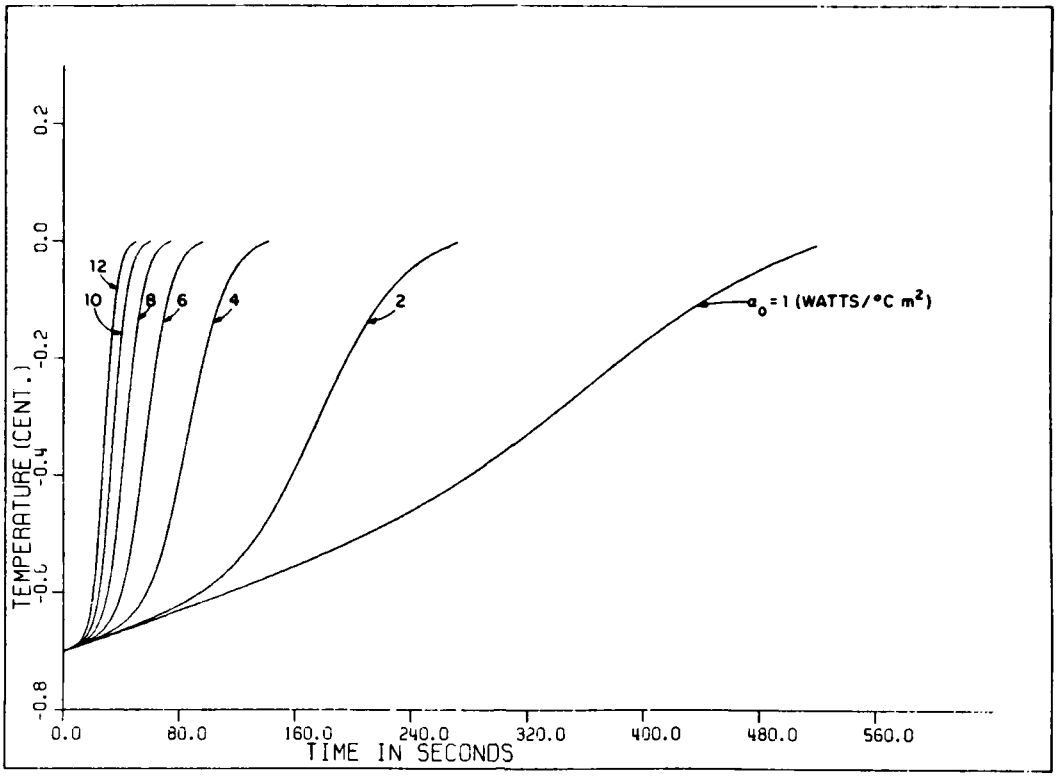

b. $T_o = -0.70°C$.

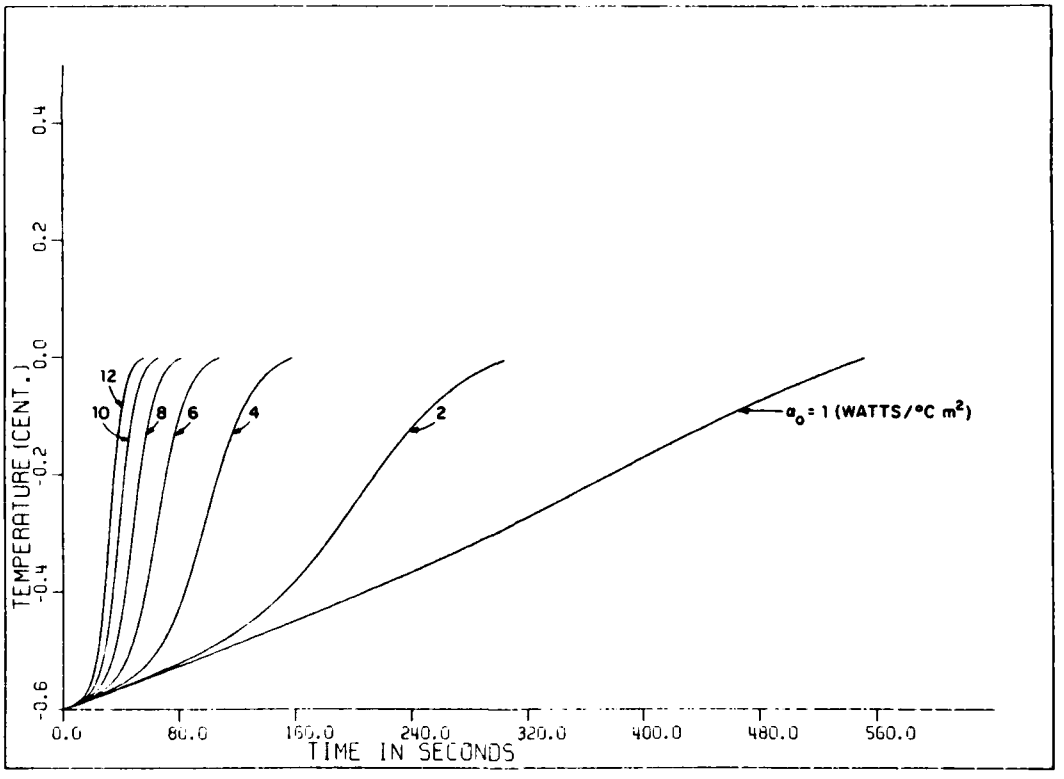

c. $T_o = -0.60°C$.

Figure C1 (cont'd). Variation of temperature rise attributable to frazil ice formation with initial value of heat transfer coefficient, α_o. *Initial temperature of supercooling is* T_o.

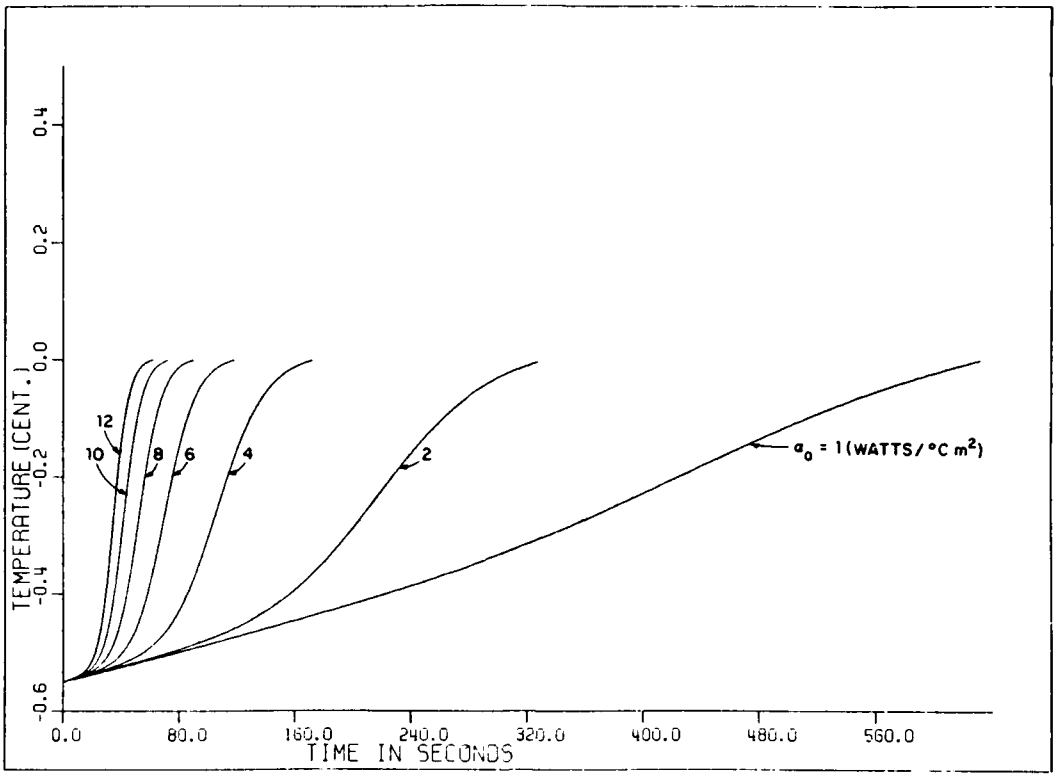

d. $T_o = -0.55°C$.

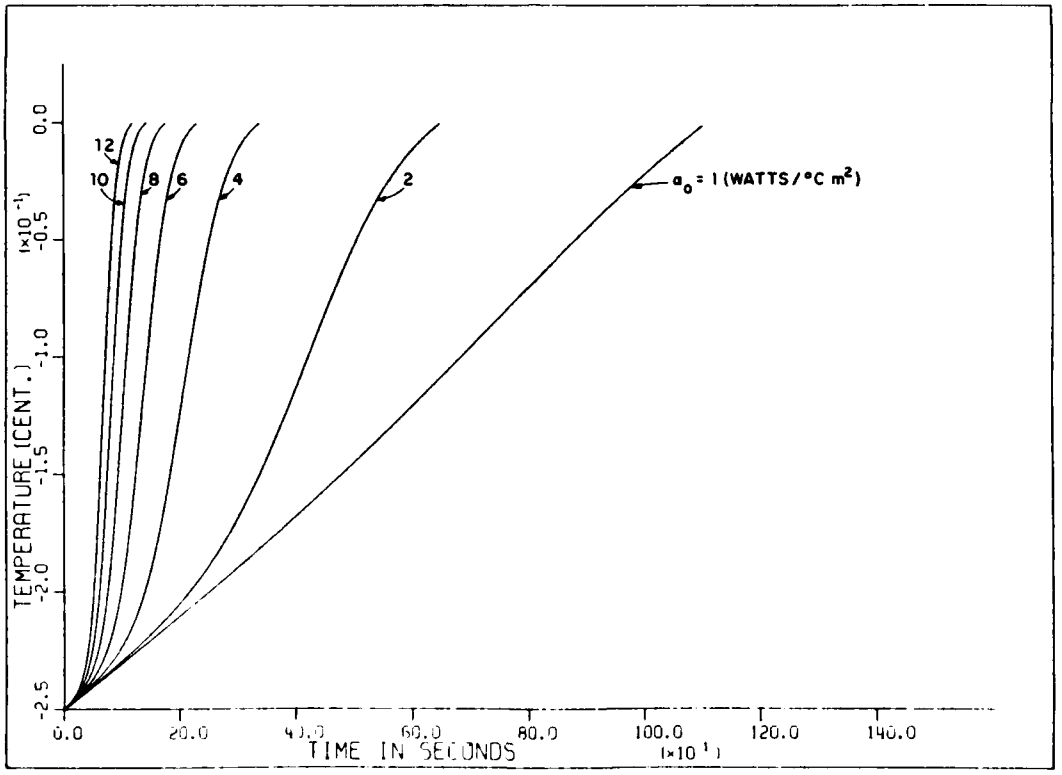

e. $T_o = -0.25°C$.

Figure C1 (cont'd).

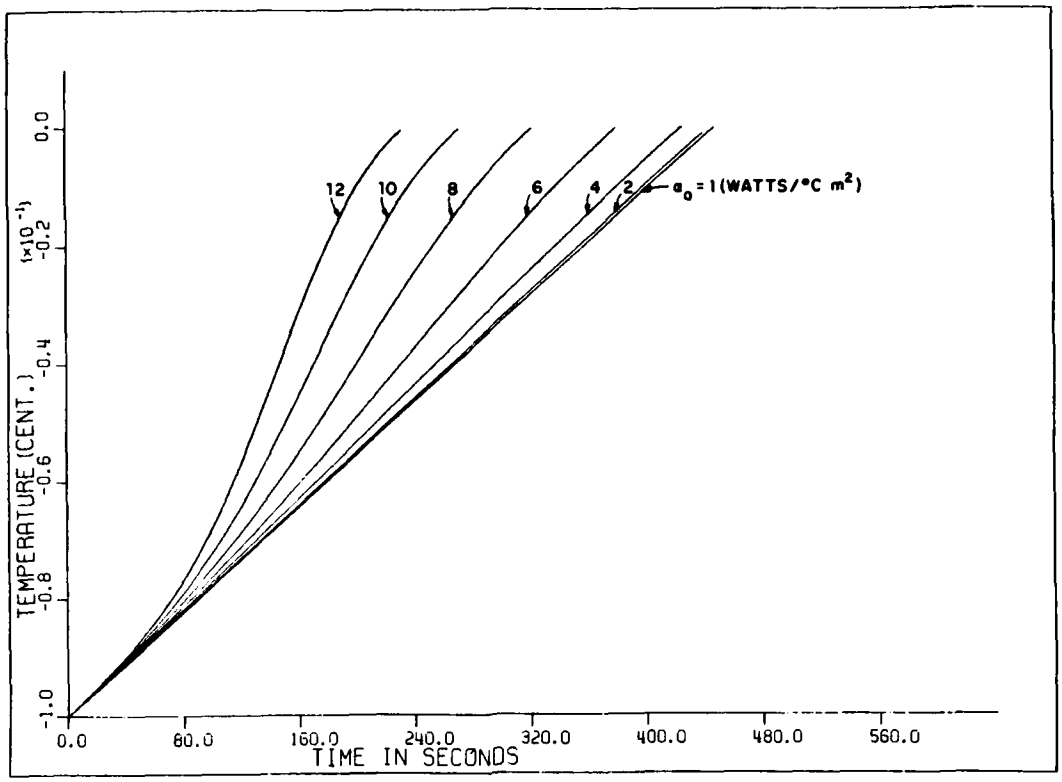

f. $T_o = -0.10°C$.

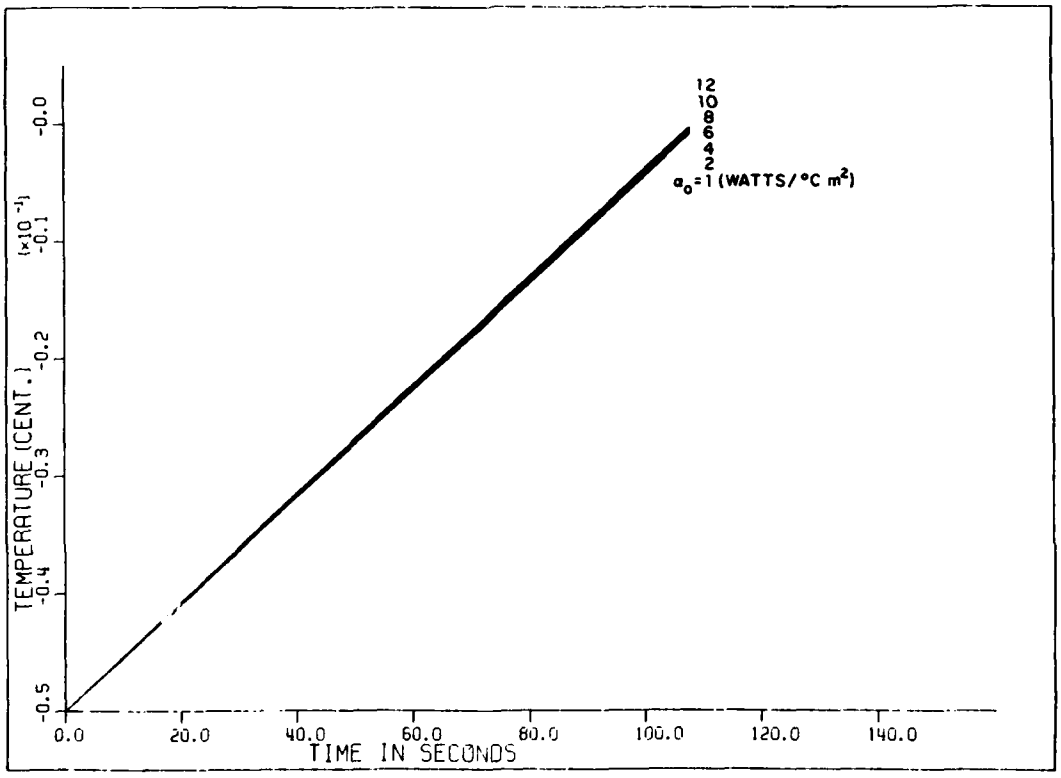

g. $T_o = -0.05°C$.

Figure C1 (cont'd). Variation of temperature rise attributable to frazil ice formation with initial value of heat transfer coefficient, α_o. *Initial temperature of supercooling is* T_o.

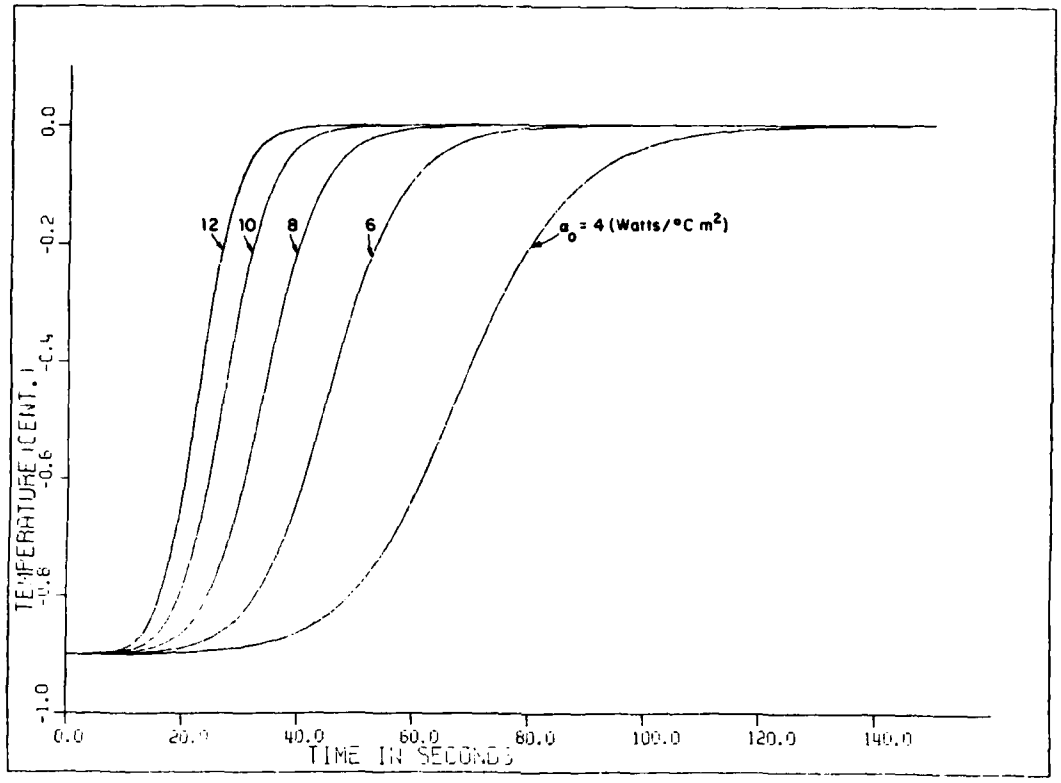

a. $T_o = -0.90°C$.

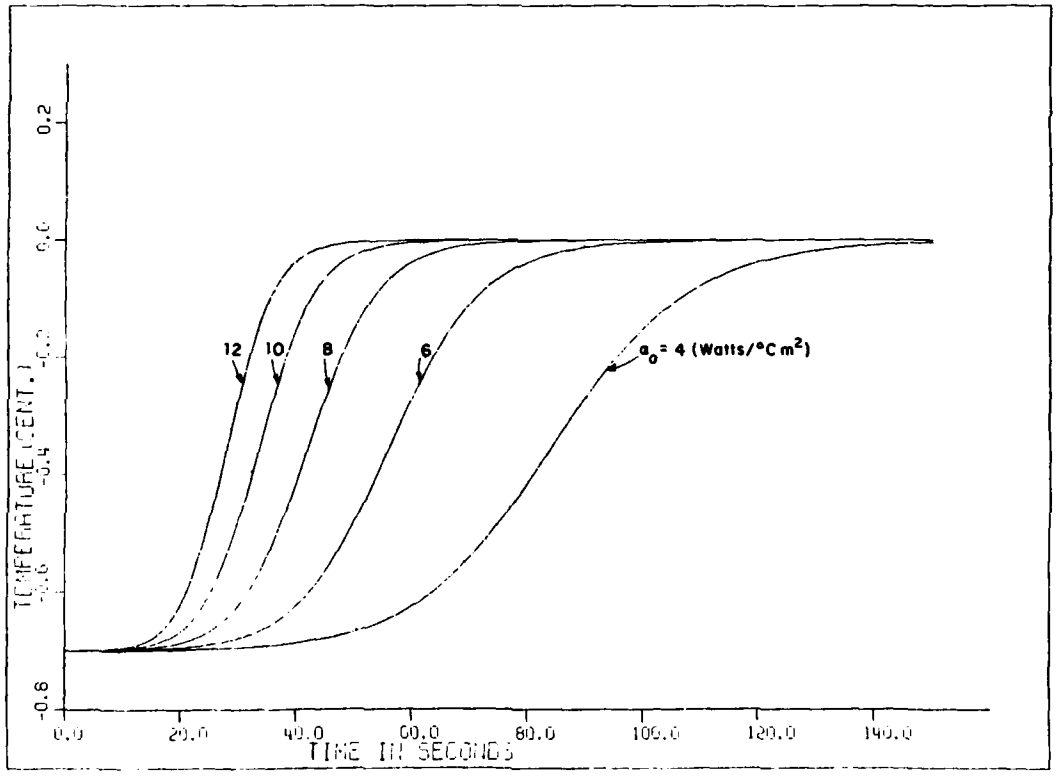

b. $T_o = -0.70°C$.

Figure C2. Variation of temperature rise attributable to frazil ice formation with initial value of heat-transfer coefficient, α_o. Grid heating $\dot{T} = 0$. Initial temperature of supercooling is T_o.

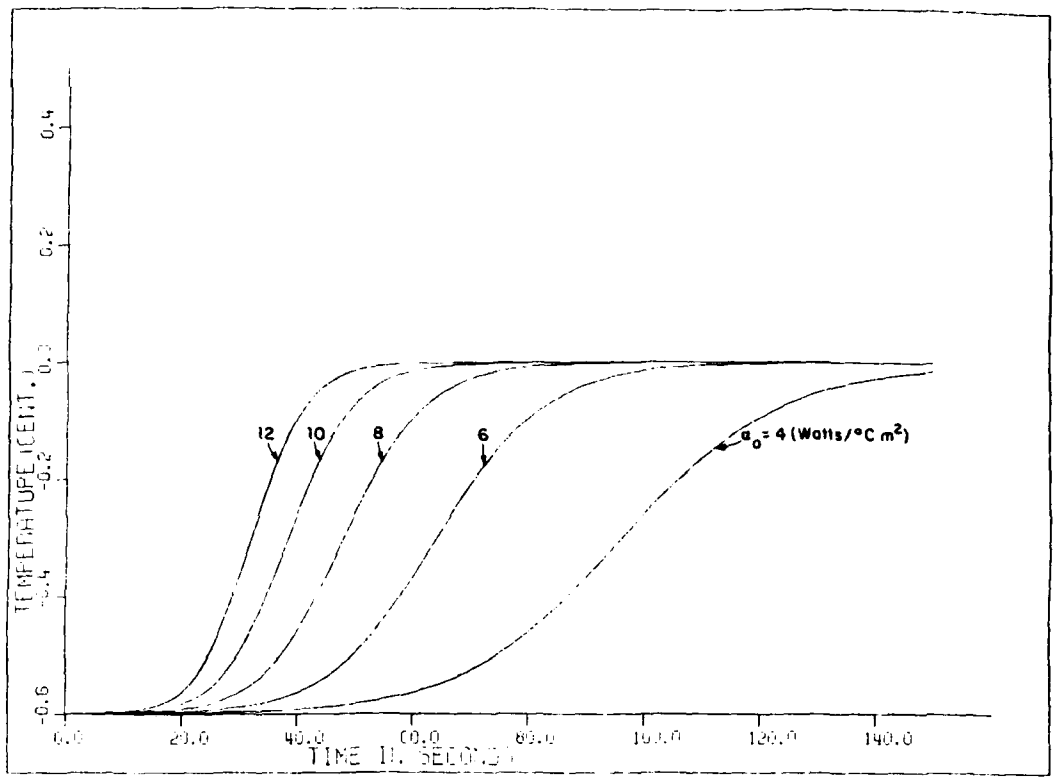

c. $T_o = -0.60°C$.

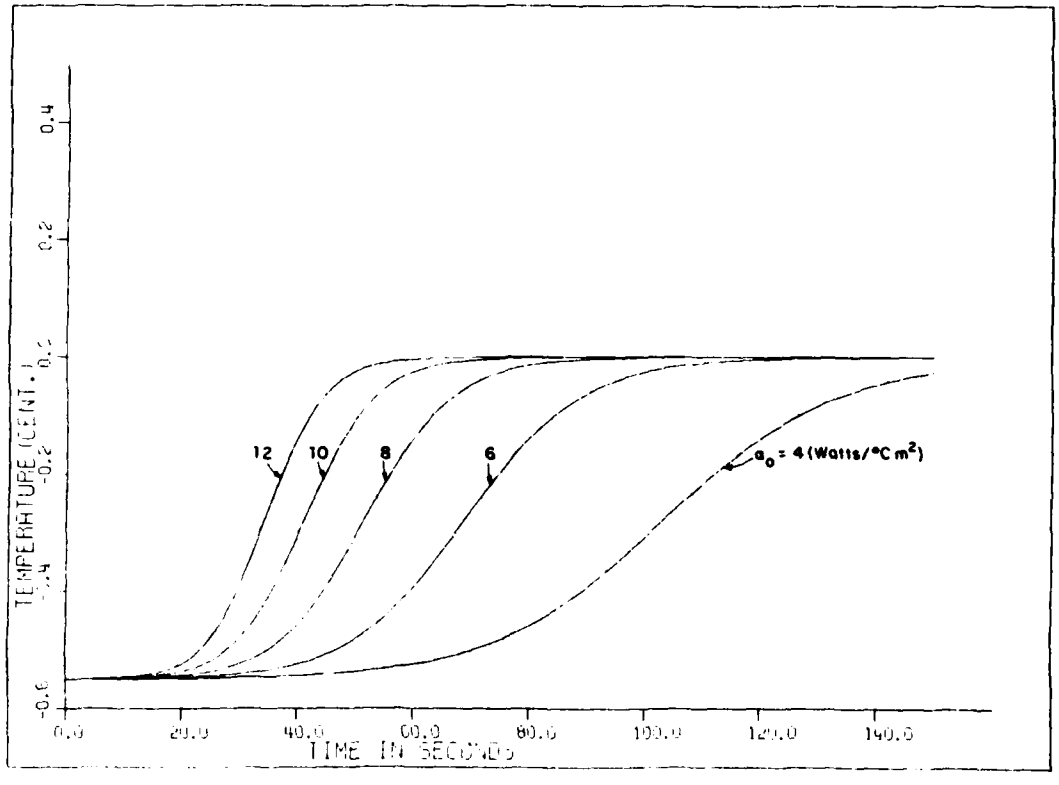

d. $T_o = -0.55°C$.

Figure C2 (cont'd). Variation of temperature rise attributable to frazil ice formation with initial value of heat-transfer coefficient, α_o. *Grid heating* $\dot{T} = 0$. *Initial temperature of supercooling is* T_o.

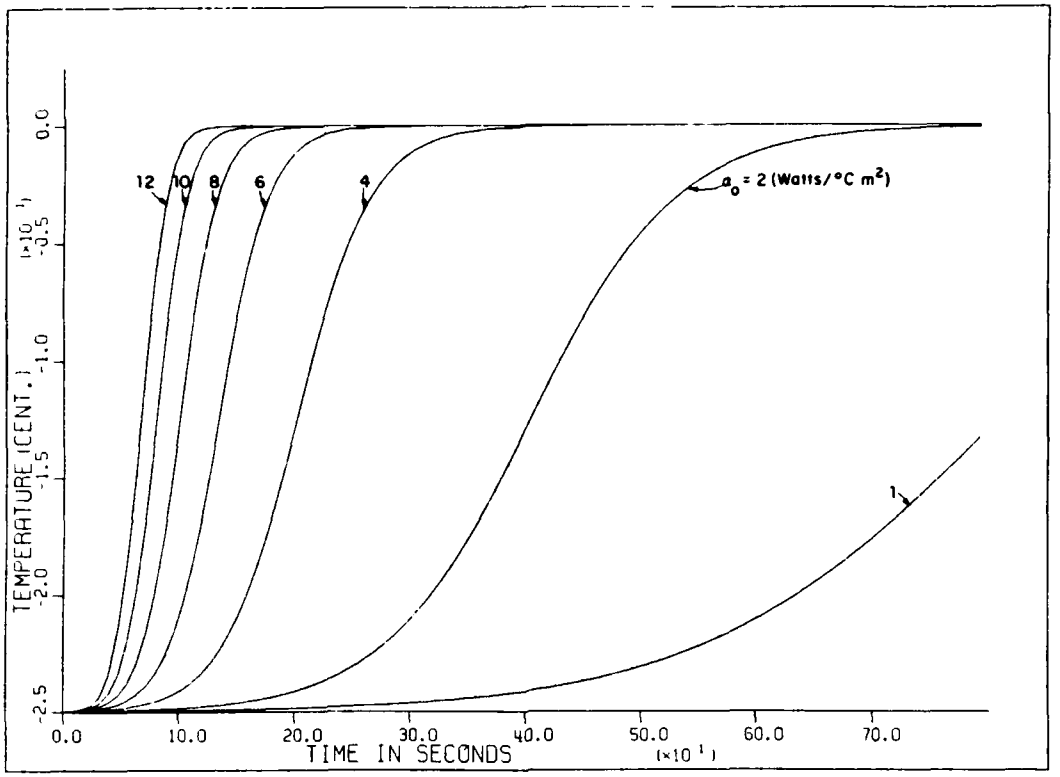

e. $T_o = -0.25°C$.

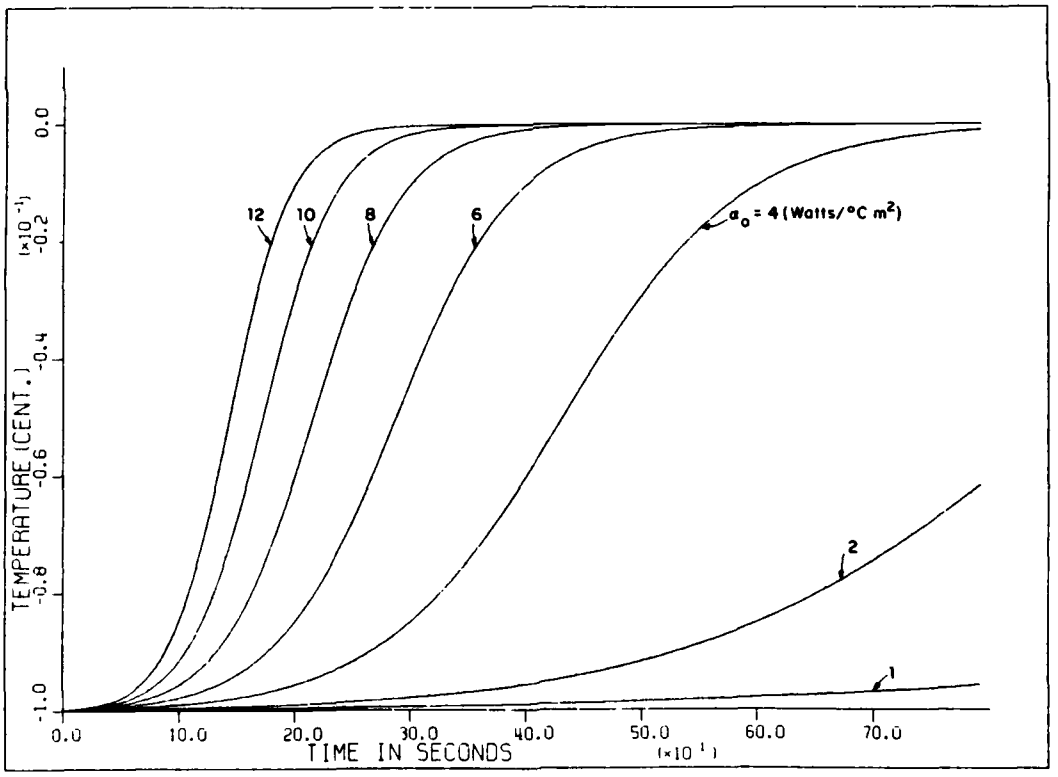

f. $T_o = -0.10°C$.

Figure C2 (cont'd).

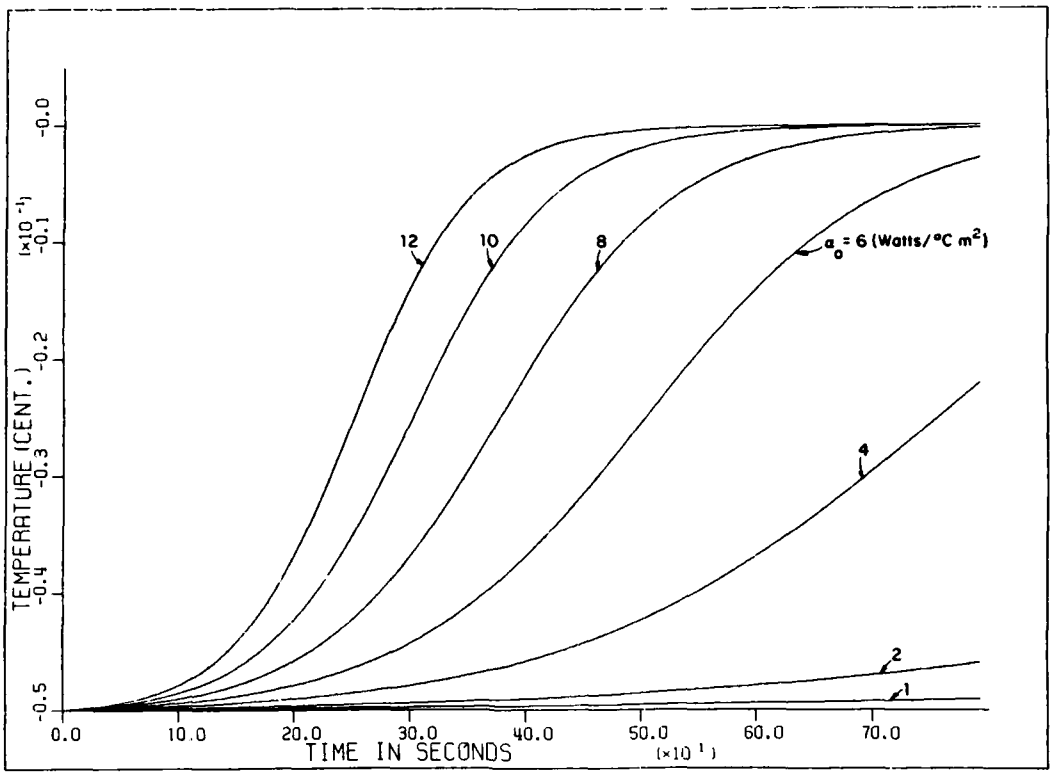

g. $T_o = -0.05°C$.

Figure C2 (cont'd). Variation of temperature rise attributable to frazil ice formation with initial value of heat-transfer coefficient, α_o. *Grid heating* $\dot{T} = 0$. *Initial temperature of supercooling is* T_o.

A facsimile catalog card in Library of Congress MARC format is reproduced below.

Ettema, R.
Frazil ice formation / by R. Ettema, M.F. Karim and J.F. Kennedy. Hanover, N.H.: U.S. Army Cold Regions Research and Engineering Laboratory; Springfield, Va.: available from National Technical Information Service, 1984.
vi, 44 p., illus.; 28 cm. (CRREL Report 84-18.)
Bibliography: p. 28.
1. Cold regions. 2. Frazil ice. 3. Ice. 4. Ice formation. 5. Laboratory tests. 6. Mathematical models. I. Karim, M.F. II. Kennedy, J.F. III. United States. Army. Corps of Engineers. IV. Cold Regions Research and Engineering Laboratory, Hanover, N.H.
V. Series: CRREL Report 84-18.

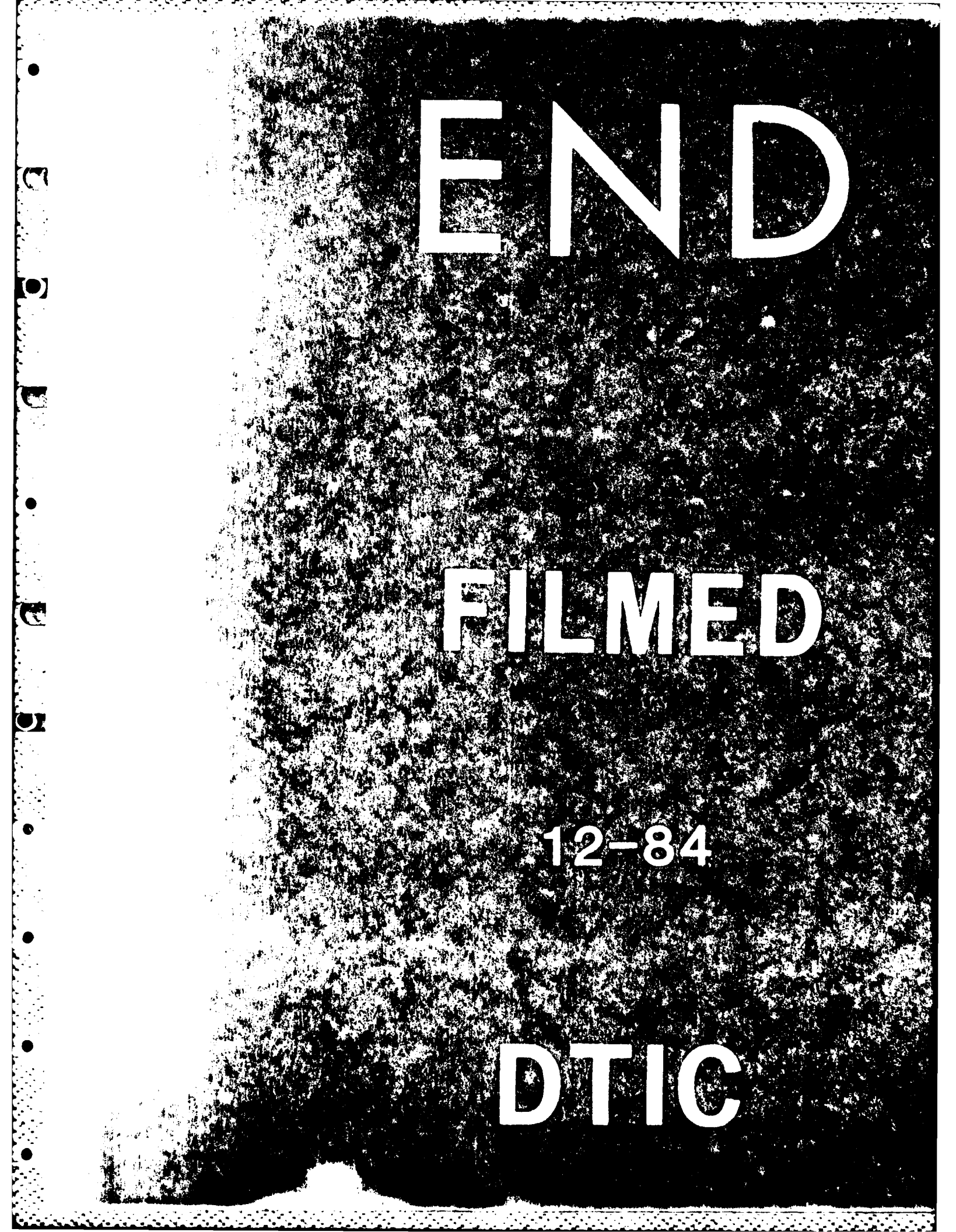
END
FILMED
12-84
DTIC